國立臺灣大學生物資源暨農學院農業化學系

碩士論文

Department of Agricultural Chemistry

College of Bio-Resources and Agriculture

National Taiwan University

Master thesis

黑色素前驅物控制阿拉伯芥鐵的吸收

Melanin precursors control Arabidopsis Fe uptake

廖小惟

Siao-Wei Liao

指導教授：盧毅 博士

Advisor: Louis Grillet, Ph.D.

中華民國 112 年 7 月

July 2023

doi:10.6342/NTU202301575

國立臺灣大學碩士學位論文

口試委員會審定書

黑色素前驅物控制阿拉伯芥鐵的吸收

Melanin precursors control Arabidopsis Fe uptake

本論文係廖小惟君(R09623003)在國立臺灣大學農業化學學系完成之碩士學位論文，於民國 112 年 6 月 19 日承下列考試委員審查通過及口試及格，特此證明

口試委員：

Louis GRILLET （簽名）

（指導教授）

doi:10.6342/NTU202301575

Acknowledgement

The two-year journey of studying the master's thesis is incredible. I have never thought about doing all the experiments and using the very data I produce myself to write a thesis. This will be my first publication! I have never dreamt of it. Within the two years of study, I have learnt useful knowledges, skills to do experiments, and several ways to deal with my nervous characteristic. I am very grateful to my advisor Prof. Louis Grillet for all his teaching and patience with me. Without his help, I can't complete a master's thesis in English. He is a nice and ambitious professor, I believe he will lead the lab to publish several wonderful papers in the near future. I'd like to thank my family, friends, and lovely lab partners who support me and tolerate me for my sometimes bad mood and willfulness. Several times I want to give up, but you are never tired of listening to me and giving me good advises that make me stand up again. Thank you with all my heart. Last but not least, I would like to thank God, for you always accompanies me.

"Do not fear, only believe." (Mark 5:36)

doi:10.6342/NTU202301575

List of Abbreviations

Abbreviation	Definition
L-DOPA	L-3,4-dihydroxyphenylalanine
IDA	Iron Deficiency Anemia
R.O. water	Reverse Osmosis water
PPFD	Photosynthetic Photon Flux Density
HPLC	High Performance Liquid Chromatography
BPDS	Bathophenanthrolinedisulfonic acid disodium salt hydrate
RT-qPCR	Real-Time Quantitative Polymerase Chain Reacion
LC-MS/MS	Liquid Chromatography-tandem Mass Spectrometry
DHI	5,6-Dihydroxyindole
DHICA	5,6-Dihydroxyindole-2-carboxylic acid
HICA	5-Hydroxyindole-2-carboxylic acid
PGPR	Plant Growth Promoting Rhizobacteria
WHO	World Health Organization

doi:10.6342/NTU202301575

摘要

不論對於動物或是植物而言，鐵都是十分重要的金屬元素。缺鐵性貧血(Iron Deficiency Anemia, IDA)是世界上很普遍的健康問題，造成 IDA 的其中一個重要原因是世界主要農作物中缺乏鐵。本研究目的旨在利用生物刺激素(biostimulant) 提升植物吸收鐵的能力以及植物種子中的鐵含量，做為增加作物鐵吸收的前期試驗。本實驗研究的生物刺激素為黑色素的前驅物左旋多巴 (L-3,4-dihydroxyphenylalanine, L-DOPA)。經過水耕試驗，可以發現 L-DOPA 雖然具有植物相剋物質 (allelopathic compound) 的特性，卻能有效的提升阿拉伯芥根部吸收鐵的能力，並且能力提升隨著施用濃度而上升。不過，完全氧化的 L-DOPA 在水耕環境中並不能促進根部鐵吸收。另一方面，土耕試驗結果顯示，澆灌 3 mM 的 L-DOPA 時阿拉伯芥種子中的鐵含量可以達到控制組的三倍之多。此外，黑色素生成路徑中除了 L-DOPA 的其他的前驅物(皆為 indolic compounds)也能夠影響阿拉伯芥的鐵吸收能力，其影響如下述：當適量供應這些 indolic compounds 且環境中的鐵充足時，阿拉伯芥的鐵吸收能力增加；反之在鐵缺乏時，阿拉伯芥的鐵吸收能力則會遭到抑制。這些結果顯示，黑色素生合成路徑上之各類化合物能顯著的影響阿拉伯芥體內鐵的動態平衡，於提升作物鐵含量之應用上具成為生物刺激素的發展潛力。

關鍵詞：鐵 (Fe)、左旋多巴 (L-DOPA)、阿拉伯芥、黑色素前驅物、缺鐵性貧血、生物刺激素、植物相剋物質

doi:10.6342/NTU202301575

Abstract

Fe is an important metallic element for both animals and plants. Fe deficiency anemia (IDA) is a common health problem worldwide, and one of the fundamental causes is the lack of Fe in the world's major crops. The purpose of this study is to use a biostimulant to enhance the ability of plants to absorb Fe and increase the Fe content in plant seeds as a preliminary test for increasing crop Fe absorption. The biostimulant studied in this thesis is L-3,4-dihydroxyphenylalanine (L-DOPA), the precursor of melanin. Through hydroponic experiments, it was found that although L-DOPA has allelopathic properties, it can effectively enhance the capability of Arabidopsis roots to absorb Fe, and the capability to absorb Fe increases with the concentration applied. However, fully oxidized L-DOPA cannot promote root Fe absorption in hydroponic environments. On the other hand, soil-based experiments showed that watering with 3 mM of L-DOPA increase the Fe content in Arabidopsis seeds to more than three folds that of the control group. In addition, other precursors of melanin in the melanin biosynthetic pathway (two of which are indolic compounds) can also affect the Fe absorption ability of Arabidopsis. When these indolic compounds are supplied in moderation with sufficient Fe in the environment, the Fe absorption ability of

doi:10.6342/NTU202301575

Arabidopsis increases; otherwise when Fe is lacked, the Fe absorption ability is inhibited. These results suggest that various compounds in the melanin biosynthetic pathway can significantly affect the homeostasis of Fe in Arabidopsis and have the potential to become a biostimulant for increasing crop Fe content.

Key words: Fe, L-DOPA, *Arabidopsis thaliana*, melanin precursors, Iron Deficiency Anemia (IDA), biostimulants, allelopathic compounds

doi:10.6342/NTU202301575

Table of Contents

口試委員會審定書……..……i

Acknowledgement ii

List of Abbreviations iii

摘要 iv

Abstract v

Table of Contents vii

List of Figures xii

List of Supplementary Tables xiv

List of Supplementary Figures xv

1. Introduction 1

1.1 Societal background: Fe is important for humans 1

1.2 Plant Fe transport and Fe homeostasis 5

1.2.1 Fe uptake from soil: strategy I and II 5

1.2.2 Regulation of Fe uptake in plants 9

1.2.3 Fe translocation from root to shoot 12

1.3 Fe biofortification crop 14

doi:10.6342/NTU202301575

1.4 The concept of biostimulants 16

1.5 L-DOPA, melanin and their relative compounds 18

1.6 L-DOPA and Fe: choosing L-DOPA as a plant Fe biostimulant 22

2. Materials and Methods 25

2.1 Plant materials 25

2.2 Chemicals used 25

2.3 Growing and harvesting hydroponic Arabidopsis 25

2.3.1 Hydroponic system 25

2.3.2 Sterilization and sowing of Arabidopsis seeds 29

2.3.3 Growth conditions 29

2.3.4 L-DOPA dissolution 30

2.3.5 L-DOPA treatment conditions 31

2.3.6 Direct germination of Arabidopsis in hydroponic system 32

2.3.7 Ferric-chelate reductase (FCR) assay 33

2.4 Arabidopsis cultivation on soil 35

2.4.1 Soil, pots, and watering 35

2.4.2 Sowing seeds onto the soil 35

2.4.3 Plant Growth conditions 36

doi:10.6342/NTU202301575

2.4.4 L-DOPA treatment 36

2.5 Fe quantification 36

2.6 Synthesis of DHICA 38

2.5 Analytical procedures 41

2.7 Analytical procedures 41

2.7.1 High-performance liquid chromatography (HPLC) 41

2.7.2 Liquid chromatography-tandem mass spectrometry (LC-MS/MS) 42

2.6 RNA analysis 43

2.8 Gene expression analysis 43

2.8.1 RNA extraction from roots 43

2.8.2 cDNA synthesis 43

2.8.3 qPCR 44

2.7 Rosette anthocyanin extraction and quantification 45

2.9 Anthocyanin extraction and quantification 45

2.9.1 Sample processing 45

2.9.2 Anthocyanin extraction 45

2.10 Fe-driven L-DOPA oxidation kinetics measurement 46

2.11 Statistical analysis 47

doi:10.6342/NTU202301575

3. Results—Part I..... 48

3.1 L-DOPA increased Arabidopsis Fe uptake in hydroponics..... 48

3.1.1 L-DOPA enhanced FCR activity of Arabidopsis roots but arrests plant growth at high concentrations..... 48

3.1.2 The allelopathic properties of L-DOPA did not cause the plant growth inhibition at low concentration in hydroponics system..... 52

3.2 qPCRs confirm L-DOPA effect on Fe uptake capacity of Arabidopsis roots.. 56

3.3 Interactions between L-DOPA and EDTA..... 58

3.3.1 L-DOPA synergistically acts with EDTA for stimulating plant Fe uptake 58

3.3.2 L-DOPA reduces free Fe (III) and gets oxidized 60

3.4 L-DOPA application increases Fe concentration in Arabidopsis rosette 62

3.5 L-DOPA increases Fe concentration in soil-grown Arabidopsis 65

3.5.1 L-DOPA decreases rosette biomass but enhances rosette Fe concentration 65

3.5.2 L-DOPA increases seed Fe content while not severely affecting seed yields..... 69

3.6 Brief discussion of Part I 72

doi:10.6342/NTU202301575

4. Results—Part II 73

4.1 L-DOPA oxidation in basic condition 76

4.2 Synthesis of high purity DHICA 81

4.3 L-DOPA and its indolic derivatives have similar effects on root FCR activity 83

4.4 Fully oxidized L-DOPA acts differently than L-DOPA 89

5. Discussion 93

5.1 L-DOPA application enables plants to take up more Fe 93

5.2 L-DOPA is not redundant with EDTA 94

5.3 L-DOPA or its oxidation products, which trigger the Fe deficiency response? 95

5.4 L-DOPA should be replenished to maintain high Fe uptake of plants 96

5.5 Novel repressors for Fe deficiency response are revealed 97

6. Conclusion 99

7. References 100

doi:10.6342/NTU202301575

List of Figures

Figure 3.1 | Root FCR activity of transferred Arabidopsis plants with a range of L-DOPA concentrations in hydroponic system……...50

Figure 3.2 | Hydroponically-grown Arabidopsis treated with series concentrations of L-DOPA for one week…….51

Figure 3.3 | Directly germinated hydroponic Arabidopsis plants treated with L-DOPA for 2 weeks…….53

Figure 3.4 | Directly germinated Arabidopsis grown for 3 weeks under low range of L-DOPA concentrations……..……54

Figure 3.5 | Root FCR activity of directly germinated Arabidopsis plants under low L-DOPA concentrations in hydroponic system……55

Figure 3.6 | Expression of *AtIRT1* and *AtFRO2* under ± L-DOPA treatments……..…..57

Figure 3.7 | Root FCR activities under ± EDTA ± L-DOPA treatments…...……59

Figure 3.8 | L-DOPA oxidation kinetics by reaction with different Fe sources…….61

Figure 3.9 | Rosette Fe concentration of plants treated with L-DOPA for 1 week…….63

Figure 3.10 | Rosette Fe concentrations of 3-week L-DOPA treated plants……..64

Figure 3.11 | Arabidopsis grown on soil and watered with different concentration of L-DOPA treatments…….....66

doi:10.6342/NTU202301575

Figure 3.12 | Rosette fresh weights of the Arabidopsis watered with L-DOPA……....67

Figure 3.13 | Rosette Fe concentrations of the Arabidopsis watered with L-DOPA…….68

Figure 3.14 | Seed yields of Arabidopsis watered with L-DOPA…….70

Figure 3.15 | Seed iron concentration of Arabidopsis watered with L-DOPA…….71

Figure 4.1 | L-DOPA oxidation process……..…….74

Figure 4.2 | Plants treated with exogenous 250 μM L-DOPA and grown at pH 5.5 and 6 under hydroponics……..76

Figure 4.4 | L-DOPA oxidation at pH 8 monitored by HPLC…….…..79

Figure 4.5 | The color changes of L-DOPA serial oxidation…….80

Figure 4.6 | Homemade DHICA has a higher purity than the commercial one……..82

Figure 4.8 | Phenotypes of Arabidopsis treated with L-DOPA, DHICA, DHI and HICA.86

Figure 4.9 | Anthocyanin concentration in rosettes of hydroponic Arabidopsis treated with L-DOPA, DHICA, DHI and HICA……..……87

Figure 4.10 | Root FCR activities of hydroponic Arabidopsis treated with L-DOPA, DHICA, DHI and HICA…….…….…….88

Figure 4.11 | Rosette biomass of Arabidopsis grown in hydroponics and subjected to L-DOPA and oxidized DOPA treatments……91

Figure 4.12 | Root FCR activity of of Arabidopsis grown in hydroponics and subjected to L-DOPA and oxidized DOPA treatments……...…...……..92

doi:10.6342/NTU202301575

List of Supplementary Tables

Supplementary Table S2.1 | Formula of the ES medium…….……28

Supplementary Table S2.2 | Settings of gradient and flow rate on HPLC…….41

Supplementary Table S2.3 | Settings of gradient and flow rate on LC-MS/MS…….....42

Supplementary Table S2.4 | Primers used for qPCR……...……..44

doi:10.6342/NTU202301575

List of Supplementary Figures

Supplementary Figure S1.1 | World prevalence of anemia in children aged 6 to 59 months, 2011……....3

Supplementary Figure S1.2 | World prevalence of anemia in pregnant women, 2011……..…….3

Supplementary Figure S1.3 | Strategy I and II of plant Fe uptake……..……...8

Supplementary Figure S1.4 | Pivotal players in Arabidopsis Fe homeostasis……..……11

Supplementary Figure S1.5 | Fe transportation between symplasm and apoplasm……13

Supplementary Figure S1.6 | The human hair DHI/DHICA ratio goes up with aging….21

Supplementary Figure S1.7 | L-DOPA triggers the expression of *IRON MAN 1* (*IMA1*/At1g47400) gene…….…….22

Supplementary Figure S1.8 | L-DOPA has Fe chelating properties…..…….....24

Supplementary Figure S2.1 | The Arabidopsis hydroponic system…….…….27

Supplementary Figure S2.2 | The homemade vacuum system for DHICA synthesis..…..39

Supplementary Figure S2.3 | A rotary evaporator was used to evaporate the solvent..….40

Supplementary Figure S4.3 | Examples of DHI dimers…….……...……73

Supplementary Figure S4.7 | DHICA and HICA……..83

Supplementary Figure S5.1 | Comparison between R3, R6, DHICA and DHI....…….98

doi:10.6342/NTU202301575

1. Introduction

1.1 Societal background: Fe is important for humans

Human beings have recognized the special role of iron (Fe) in health and disease from ancient times (O'Dell & Sunde, 1997). Until 1932 people fully understood the importance of Fe for human because by then Fe was discovered necessary for hemoglobin synthesis (Heath et al., 1932). Nowadays, the fact that Fe is an indispensable trace element for humans has been confirmed and is accepted by people around the world.

Fe has several vital functions in human body — The Fe-containing hemes in red blood cells can carry oxygen from lungs to tissues; Fe-sulfur clusters participate in the electron transport chain of cellular respiration in the mitochondria; finally, Fe is a cofactor of several important enzymes, for example, it is a component of the catalase which discomposes hydrogen peroxide to water and oxygen (Scibior & Czeczot, 2006; Gupta, 2014).

To have Fe functions inside human body, Fe has to be absorbed through our daily diet. There are two chemical groups of dietary Fe which can be taken up by humans: heme Fe and non-heme Fe. Heme Fe is derived from metalloprotein—hemoglobin and myoglobin of animal food sources like meat or poultry. Heme Fe is the most

doi:10.6342/NTU202301575

bioavailable form of Fe for human intestine, and accounts for over 10 % of total dietary Fe absorption (Ems et al., 2021). Non-heme Fe predominantly derives from plants and Fe-fortified foods like animal tissues or egg yolk. Non-heme Fe plays a subordinate role in human nutrition because of its low bioavailability (Hurrell & Egli, 2010), but non-heme Fe is the most abundant form of Fe in most diets, with a concentration several fold higher than heme Fe (Monsen et al., 1978).

Despite the essential role of Fe and its relative abundance in food, many people worldwide do not obtain sufficient Fe through their diet to maintain their health. Fe deficiency anemia (IDA) is the most prevalent nutritional disorder in the world (Denic & Agarwal, 2007) affecting approximately 1 billion people (Stoltzfus, 2003).

The common symptoms of IDA in adults include reduced work capacity, impaired thermoregulation, immune dysfunction, glycemic index (GI) disturbances, migraine and depression, and increasing the risk of bacterial infection (Beard, 2001; Haas & Brownlie IV, 2001; Oppenheimer, 2001; Franceschi & Gasbarrini, 2007; Pamuk et al., 2016). In young children, IDA leads to psychomotor disabilities and retarded learning (Beard, 2003; Lozoff et al., 2007). In pregnant women, IDA has long been associated with low birth weight of a newborns, preterm delivery, perinatal mortality, and infant as well as maternal mortality (Brabin et al., 2001; Rasmussen, 2001).

doi:10.6342/NTU202301575

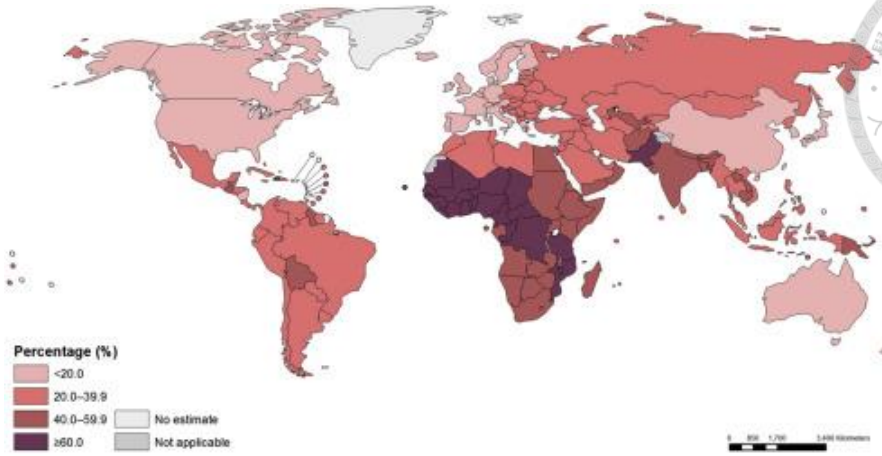

Supplementary Figure S1.1 | World prevalence of anemia in children aged 6 to 59 months, 2011.

Anemia is a serious health problem in the population of children of developing countries. (Source: WHO database on anemia)

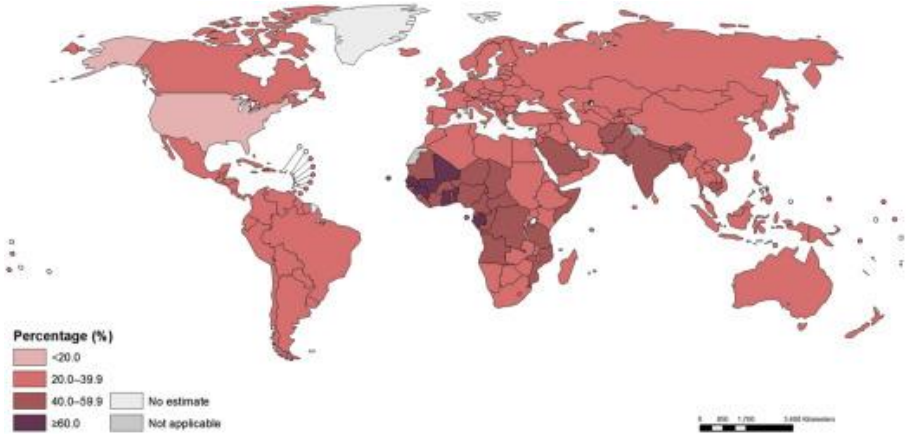

Supplementary Figure S1.2 | World prevalence of anemia in pregnant women, 2011. Anemia is a prevalent phenomenon for pregnant women around the world which incurs serious risks for them. (Source: WHO database on anemia)

doi:10.6342/NTU202301575

Fe is the most abundant metal element on Earth and the most commonly utilized transition metal in the biosphere (Kappler & Straub, 2005). It is also the fourth most abundant element in the crust of Earth (Frey & Reed, 2012). If these are the cases, why do so many people in the world still suffer from IDA? Humans rely heavily on non-heme Fe which derived predominantly from plants to maintain health, the soil where world major crops are grown, however, have low Fe bioavailability. Fe presents mainly in the form of Fe (III) in the soil, which is only scarcely soluble under aerobic conditions, especially in neutral and high pH soils (Marschner, 1995; Hindt & Guerinot, 2012). Fe deficiency and Fe chlorosis in crops are commonly associated with calcareous soils with high pH (Loeppert & Hallmark, 1985). Unfortunately, calcareous soils are widely spread in arid and semiarid regions in the world. These calcareous soils occupy more than one-third of the world's land surface area (Taalab et al., 2019). The high pH of the calcareous soils seriously limits the Fe plants acquire from the soil thus impede humans and livestock from acquiring ample Fe from crops and fodders.

Fe deficiency can cause crop growth difficulty for sure. It is reported that in the Western half of the U.S., where the soils are drier and more alkaline, crops like soybean, maize and sorghum undergo severe Fe deficiency and even cannot be grown. Though it is hard to estimate the economic losses Fe deficiency brings about in this region when

doi:10.6342/NTU202301575

other factors such as water and special climate conditions may be more important (Clark, 1982), Fe deficiency is definitely more of a problem than generally believed.

1.2 Plant Fe transport and Fe homeostasis

Fe is not only important for humans and animals but also important for plants. It is a trace element which is involved in all growth stage of a plant. Fe participates in a great number of biochemical processes such as photosynthesis, chlorophyll synthesis, enzyme production, and respiration. Excess and shortage of Fe leads to Fe toxicity and Fe deficiency, respectively.

According to International Plant Nutrition Institute (IPNI), the Fe concentration in plant leaf varies between species, but is commonly between 50 and 250 ppm (dry weight basis). If Fe concentration in leaf tissue is less than 50 ppm, there are usually signs of deficiency, and toxic effects can be observed when the Fe concentration in the leaves exceeds 500 ppm.

1.2.1 Fe uptake from soil: strategy I and II

There are two strategies for plants to uptake Fe. Strategy I is adopted by nongraminaceous plants and strategy II is adopted by graminaceous plants (Römheld & Marschner, 1986). The two major processes in strategy I are the reduction of Fe (III) at the root surface and the absorption of the generated Fe (II) through the transporters on

doi:10.6342/NTU202301575

root plasma membrane. The ferric-chelate reductase oxidase FRO2 is responsible for the reduction of Fe (III) to Fe (II), and the IRON-REGULATED TRANPORTER 1 (IRT1) is responsible for importing Fe (II) into the plant roots (Eide et al., 1996). As mentioned above, Fe has low mobility at high pH, therefore plants evolved H^+-ATPase (HA) genes which mediate proton extrusion to facilitate iron solubilization, and can be induced when Fe is not available. In Arabidopsis, for example, the HA protein AHA2 is responsible for lowering the pH during Fe deficiency to increase Fe bioavailability (Santi & Schmidt, 2009). The release of phenolic compounds in the rhizosphere by plants with limited Fe source was suggested as another alternative that facilitates Fe mobilization and uptake by plant roots (Römheld & Marschner, 1983). Several studies in Arabidopsis reveal the Fe-mobilizing phenolics are root-secreted coumarins and they have an important role in plant Fe acquisition in high pH soil where the mobility of iron is low (Schmidt et al., 2014; Fourcroy et al., 2016; Rajniak et al., 2018). Coumarins participate in Fe acquisition by chelation of Fe (III) which is subsequently reduced to Fe (II) by FRO2 and transported into the root via transporter IRT1 (Schmid et al., 2014; Schmidt et al., 2014; Sisó-Terraza et al., 2016).

The coumarin use by Arabidopsis is similar to strategy II adopted by graminaceous plants, which is also known as the "chelation strategy" since it consists in the secretion of molecules with high Fe affinity that enhance Fe solubility. Strategy II Fe uptake

doi:10.6342/NTU202301575

relies on biosynthesis and secretion of mugineic acids (MAs), which are specific to graminaceous plants. MAs are called phytosiderophores (PSs) due to their high affinity for Fe (III). So far, nine types of MAs have been identified. (Mori & Nishizawa, 1987; Shojima et al., 1990; Ma et al., 1999; Bashir et al., 2006; Ueno et al., 2007). In the synthesis pathways of MAs, there are three sequential enzymes which are in common—NICOTIANAMINE SYNTHASE (NAS), NICOTIANAMINE AMINOTRANSFERASE (NAAT), and DEOXYMUGINECI ACID SYNTHASE (DMAS). With the very precursor of these reactions being *S*-adenosyl-L-methionine, the product of these three sequential enzymes is 2'- deoxymugineic acid (DMA), which is the precursor of all other MAs (Kobayashi & Nishizawa, 2012). The MAs are secreted into the rhizosphere by the transporter TOM1. After they enter the rhizosphere, MAs solubilize Fe (III), and the resulting Fe(III)-MA complexes are taken up into root cells by the YS and YSL transporters.

doi:10.6342/NTU202301575

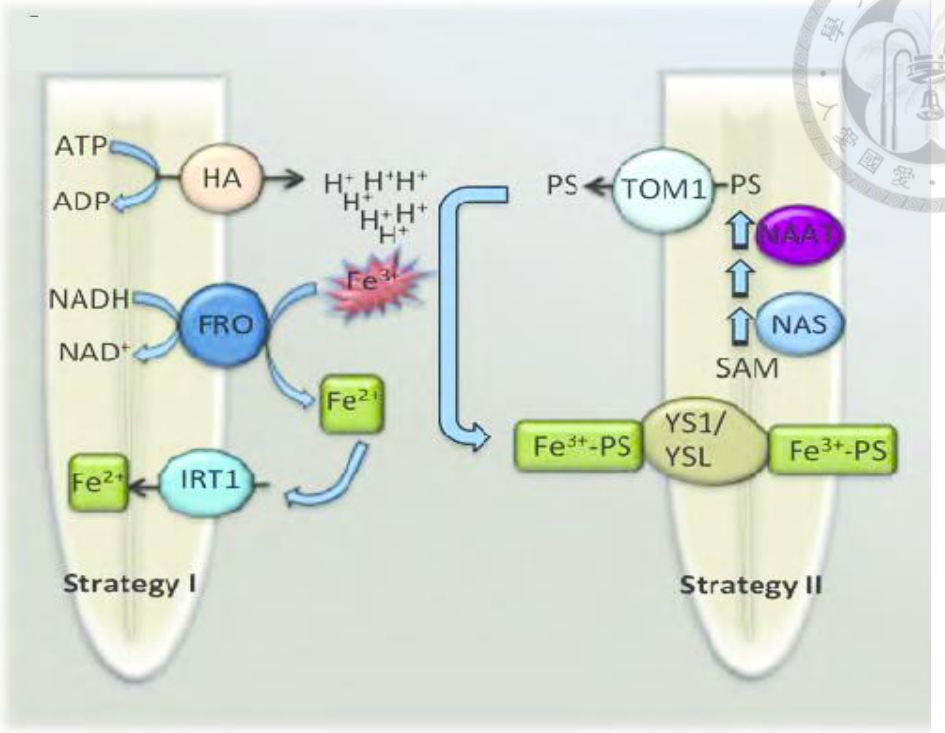

Supplementary Figure S1.3 | Strategy I and II of plant Fe uptake . Strategy I is used by non-graminaceous plants. Non-grass plants can secrete hydrogen ion through HA to the environment to increase the bioavailability of iron. The iron form in the environment is majorly iron (III). It is sequentially reduced by root FRO2 into iron (II) and finally taken up by root through transporter IRT1. Strategy II is for graminaceous plants. Graminaceous plants secrete PS to chelate iron (III) and then transport the complex back into the root by YS1 and YSL transporters. HA, H^+-ATPase; FRO2, ferric-chelate reductase oxidase 2; IRT1, iron-regulated transporter 1; PS, phytosiderophore; YS1, Yellow Stripe 1; YSL, Yellow Stripe 1-Like (López-Arredondo et al., 2013).

doi:10.6342/NTU202301575

1.2.2 Regulation of Fe uptake in plants

In the model plant Arabidopsis, the mechanism of regulation of Fe uptake is partly established. Uptake of Fe is controlled by a complex network of *trans*-acting factors, regulatory peptides and ubiquitin ligases. There are 2 situations: Fe sufficient and Fe deficient.

When Fe is sufficient, the Fe uptake is switched-off at the transcriptional level. Under Fe deficiency, the transcription factors UPSTREAM OF IRT1 (URI)/bHLH121 heterodimerize with other bHLH transcription factors of the subgroup IVc (IAA LEUCINE RESISTANT 3 (ILR3) /bHLH105, IRON DEFICIENCY TOLERANT 1 (IDT1)/bHLH34, bHLH104 and bHLH115). These heterodimers bind to the promoters of *Fe DEFICIENCY INDUCED TRANSCRIPTION FACTOR 1 (FIT1)/bHLH29* and *bHLH* subgroup *1b*, producing transcription factors that in turn activate the transcription of the Fe uptake genes *FRO2* and *IRT1*. As plants take up more Fe and become Fe-replete, the Fe binding E3 ligase BRUTUS (BTS) mediates the targeting of bHLH IVc proteins to the proteasome, thereby destabilizing the heterodimer composed of URI/bHLH121 and bHLH IVc and effectively switching off the Fe deficiency response.

When iron is scarce, the IRONMAN peptides (IMAs), notably IMA3, interact with BTS and prevent the bHLH IVc degradation by serving as dummy target for BTS. As the plant increases its Fe uptake and Fe makes its way into cells, ferrous ions bind to

doi:10.6342/NTU202301575

BTS and destabilize it. URI activity is also modulated by phosphorylation, and its phosphorylated form is able to trigger the Fe deficiency signaling cascade described above, and ultimately Fe uptake (Li et al., 2021; Vélez-Bermúdez & Schmidt, 2022). The mechanism triggering the phosphorylation of URI remains unknown, as well as how it is controlled. FIT/ bHLH29 is another key player in Arabidopsis Fe homeostasis. FIT is downstream of URI but upstream of Fe uptake genes like *IRT1*, *FRO2* and *AHA2*. FIT is indirectly regulated by URI (Gao et al., 2020). URI phosphorylation activates bHLH Ib expression, the bHLH Ib proteins subsequently form heterodimers with FIT to upregulate the transcription of genes mediating the acquisition of Fe from the soil. There are BRUTUS-LIKE 1 (BTSL1) and BTSL2 in Arabidopsis which are induced under Fe deficiency, targeting FIT for degradation. While the small peptide IMA1 reportedly prevents FIT from being degraded by BTSLs thereby preventing inhibition of Fe uptake (Lichtblau et al., 2022).

doi:10.6342/NTU202301575

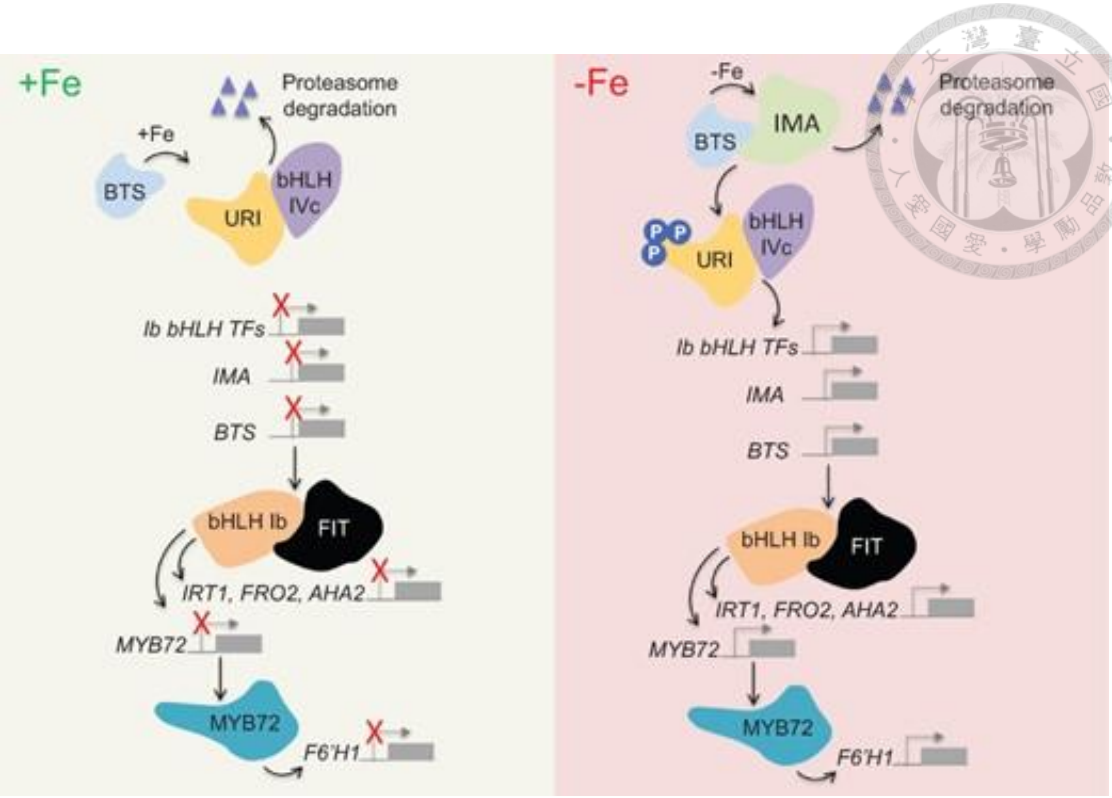

Supplementary Figure S1.4 | Pivotal players in Arabidopsis Fe homeostasis.

URI/bHLH121 complexes with ILR3 and other clade IVc bHLH proteins to regulate downstream genes. In the absence of Fe, phosphorylation (indicated in blue bubbles) activates URI, promoting the binding of its targets. E3 ubiquitin ligase BTS mediates proteasomal degradation of transcription factor complexes to turn off Fe signaling when Fe is available. IMA peptides induce the transcription of downstream genes by competing for BTS binding in the absence of Fe. FIT is indirectly regulated by URI. Clade Ib bHLH proteins form heterodimers with FIT to upregulate the transcription of *AHA2*, *FRO2*, and *IRT1*. Transcription of *MYB72* is also induced by FIT/bHLH Ib heterodimer to regulate the production and secretion of coumarins, aiding Fe acquisition at elevated pH (Vélez-Bermúdez & Schmidt, 2022).

doi:10.6342/NTU202301575

1.2.3 Fe translocation from root to shoot

After Fe being taken up into the plant roots, various Fe chelators prevent Fe precipitation inside cells and formation of detrimental reactive oxygen species (ROSs) through Fenton reactions. The best described chelators are nicotianamine (NA), citrate, malate and deoxymugineic acid (DMA).

In model plant Arabidopsis, Fe is translocated from roots to shoots by bulk flow through the xylem as ferric Fe complexed to citrate, malate or both. In the cell apoplast, Fe (III) can be easily reduced to Fe (II) by light, extracellular ascorbate or by FRO family reductase localized at the plasma membrane. The highly reactive Fe (II) is fairly unstable and requires chelation by NA. Fe (II)-NA can readily circulate through the symplasmic path and load into the phloem through plasmodesmata. Free Fe (II) rapidly oxidizes to Fe (III). In the relatively basic phloem, Fe (II) is believed to be predominantly bound to NA. NA can also bind to Fe (III) but the Fe (III)-NA complex is not stable in the xylem where the pH is only 5.5 (Timberlake, 1964). In sink organs, Fe (II)-NA can exit the phloem via plasmodesmata, or diffuse out of the phloem into the apoplasm and is retrieved into symplasm by YSL or oligopeptide transporter (OPT) (Grillet et al., 2014).

doi:10.6342/NTU202301575

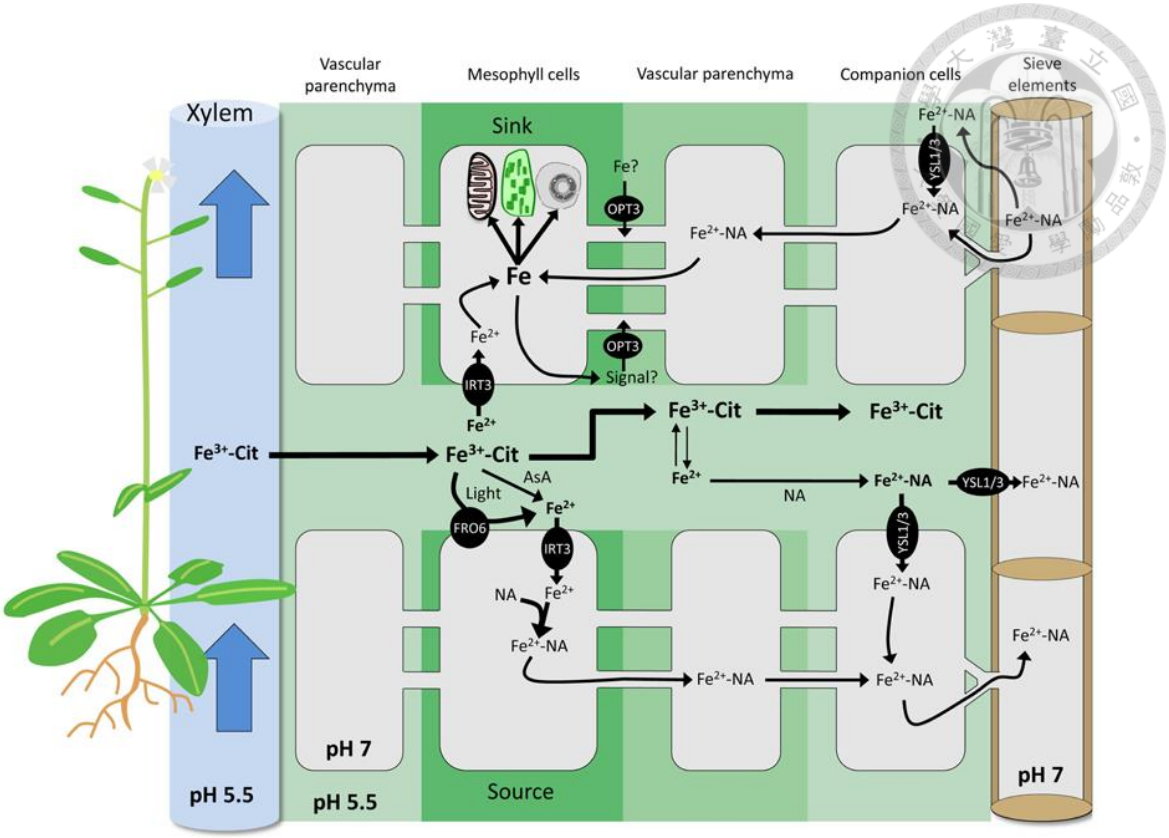

Supplementary Figure S1.5 | Fe transportation between symplasm and apoplasm.

Overall, the movement and regulation of Fe in plants are complex processes that involve multiple transporters and mechanisms. The conversion of Fe (III) to Fe (II) by FRO6, the alternation between Fe-NA and Fe-citrate complexes in phloem and xylem, and the role of YSL transporters and OPT3 in the uptake and circulation of Fe all contribute to the efficient distribution of this essential nutrient throughout the plant. Further research is needed to elucidate the precise signaling pathways and regulatory mechanisms that govern these processes. AsA, ascorbic acid; Cit, citrate; FRO, Ferric Reductase Oxidase; IRT, Iron-Regulated Transporter; NA, nicotianamine; OPT, OligoPeptide Transporter; YSL, Yellow Stripe-Like. (Grillet et al., 2014)

doi:10.6342/NTU202301575

1.3 Fe biofortification crop

How to increase Fe content in edible plants? Humans have come up with various plans to fight low Fe content in crops and vegetables for a long time. Crop breeding is a classic and effective method throughout history. But for a fairly long time, people had pursued yield increase and good disease resistance of crops therefore the issue of nutrient composition inside the grains of main staple food had been neglected. Modern varieties of wheat and rice have a lower concentration of Fe in grains than traditional varieties (Graham et al., 1999; Ortiz-Monasterio & Graham, 1999). Now scientists manage to rescue the low Fe content in grains also by breeding. Cakmak *et al.* once demonstrated in 2000 that the chromosomes 6A and 6B of wild tetraploid wheats (ssp *dicoccoides*) possess valuable genes responsible for high levels of Fe and Zn in seeds. These lines can therefore be used to enhance the grain content of Fe and Zn in contemporary hexaploid wheat (ssp *aestivum*) (Cakmak et al., 2000). Another practical example to increase crop Fe content by breeding is the case of high Fe rice variety IR68144. This rice cultivar has high yield, decent tolerance to mineral deficiency, and good disease tolerance. IR68144 was developed through the crossing between a semi-dwarf and high-yielded rice cultivar—IR8, and Taichung (Native)-1 (Kok et al., 2018).

Even though traditional breeding successfully led to the development of cultivars

doi:10.6342/NTU202301575

with high yield and high Fe content, this method alone is very slow and always has a difficulty to maintain a good balance between yield and quality (Graham et al., 1999).

Increasing plant Fe content by agronomic practice is another good option. Soil conditions such as pH, aeration, soil composition, and soil water content are important for Fe availability and Fe uptake in plants (Prasad et al., 2014; De Valença et al., 2017). Soil properties can be changed by application of organic wastes such as animal manure and plant residues. Organic waste can decrease soil pH, enhance cation exchange capacity and Fe bioavailability; it also provides a more constant and slower nutrient release compared to traditional fertilizers (Zingore et al., 2008). However, application of organic wastes alone is insufficient to alleviate Fe deficiency. If getting rid of plant Fe deficiency is the final target, it requires combined application of organic waste and Fe fertilizer (De Valença et al., 2017). Fe fertilizer can be applied directly onto the leaves of the plants, or to the soil.

Even though application of Fe fertilizer brings convenience for plants to uptake Fe, the fertilizer can't stick to the foliars of plants and is often removed by rain. Reapplication of Fe fertilizer after rain is always needed, which is too costly (García-Bañuelos et al., 2014; De Valença et al., 2017).

The third way to enhance crop Fe content is through genetic engineering. Compared to agronomic practices and conventional plant breeding, genetic engineering

doi:10.6342/NTU202301575

technologies provide a more efficient and reliable way to study the relationship between genotypes and phenotypes (Lei et al., 2020). Genetic engineering methods are therefore preferred alternatives for biofortification to increase Fe content in crops and have been successful in the past. For example, a group of researchers increased rice Fe storage by introducing *ferritin* genes from soybean to enhance the expression of ferritin, a Fe storage protein which is capable to store up to 4500 Fe (Goto et al., 1999; Theil, 2003). In another study, *NAS* genes were overexpressed in rice to achieve Fe biofortification. NAS catalyze the synthesis of the Fe chelator nicotianamine and the enhanced expression of *NAS* genes can increase the translocation and the content of Fe and zinc in crops such as soybean, rice and sweet potato (Nozoye, 2018).

Despite the many examples showing the merits of using genetic engineering to increase crop Fe content, doubts about health risks that genetically modified crops might bring about preclude their widespread adoption (Dona & Arvanitoyannis, 2009).

1.4 The concept of biostimulants

The methods introduced above for Fe biofortification all have their advantages and drawbacks, and the ideal solution are likely to lie in a combination of strategies. In the present study, we propose to use a relatively novel approach by using “biostimulants”.

What are biostimulants? Biostimulants are defined in 2007 as materials, other than

doi:10.6342/NTU202301575

fertilizers, which promote plant growth when applied in low quantities (Kauffman et al., 2007). Later in 2015, a newer definition for biostimulants comes out — "A plant biostimulant is any substance or microorganism applied to plants with the aim to enhance nutrition efficiency, abiotic stress tolerance and/or crop quality traits, regardless of its nutrient content (Du Jardin, 2015)". For example, microbial inoculants can be considered as plant biostimulants for their abilities to increase the supply of nutrients and root area, and enhance nutrient uptake capacity of the plant in a relative low quantity (Vivas et al., 2003; Calvo et al., 2014).

Are there any substances which can serve as biostimulants for plant Fe uptake? Recently, some innovative materials have been found or produced to serve as biostimulants for this aim. Humic substances (HS) extracted from different soil sediments and solutions were reported to be novel and effective biostimulants for plant Fe nutrition uptake (Zanin et al., 2019). In 2021, a study pointed out that synthetic proline-2'-deoxymugineic acid, an analog to Poaceae naturally secreted synthetic 2'-deoxymugineic acid which can rescue Fe deficiency symptoms in rice grown in calcareous soil, has great potential to be used as rice Fe biostimulant at alkaline soils with a relatively friendly cost and higher stability (Suzuki et al., 2021).

Besides materials mentioned above, scientists are still searching for more and more compounds potent of being good plant Fe uptake biostimulants. A screening of

doi:10.6342/NTU202301575

chemical compounds library revealed that some molecules have opposite bioactivities. Two compounds called R3 (N-[4-(1,3-benzothiazol-2-yl)-2-methylphenyl] acetamide) and R6 (2-benzoyl-1-benzofuran-5-carboxylic acid), reportedly blocked the activation of Fe deficiency responses in *Arabidopsis thaliana* (R stands for "repressor of IRT1) (Kailasam et al., 2019). Although these molecules were found to repress rather than stimulate Fe uptake, they still help in elucidating the plant Fe uptake regulatory mechanisms.

The main scope of this thesis is testing the ability of a non-proteinogenic amino acid, L-DOPA, which is the precursor of the ubiquitous pigment melanin, to stimulate plant Fe uptake. The rationale behind the choice of L-DOPA as a biostimulant for plant Fe uptake is discussed in paragraph 1.6, following a formal introduction of L-DOPA.

1.5 L-DOPA, melanin and their relative compounds

L-3,4-dihydroxyphenylalanine (L-DOPA) is a non-protein amino acid produced from tyrosine hydroxylation. It is a precursor of several biologically active compounds such as the catecholamine neurotransmitters dopamine and epinephrine. Catecholamines are amines with a 3,4-dihydroxy-substituted phenyl ring. Dopamine can be generated through L-DOPA decarboxylation. L-DOPA can also further form noradrenaline and adrenaline through hydroxylation and methylation. (Steiner et al., 1996; Kong et al.,

doi:10.6342/NTU202301575

1998; Kulma & Szopa, 2007).

Melanins are the final products of spontaneous oxidation of L-DOPA. Melanins are non-homogenous light-absorbing polymers which contain indoles and other intermediate products derived from the oxidation of phenolic compounds. They are a group of pigments widely spread in animal, bacteria and fungi kingdoms (Riley, 1997). Melanins contribute not only to the dark color formation in surface structures of vertebrates, but are also important for protecting animal skin from harmful UV light, hardening the exoskeleton of insects, enhancing the survival of fungi during infection of other pathogenic fungi and protecting against Reactive Oxygen Species (ROS) (Ozeki et al., 1997; Riley, 1997; Sugumaran, 2002; Gessler et al., 2014). In plants, melanin is considered to be mostly allomelanin, a structurally different form of melanin mostly constituted of coumaric acid, in contrast to the most widespread L-DOPA-derived eumelanin.

L-DOPA constitute the main treatment against human Parkinson's disease, a neurodegenerative disorder which is characterized by the loss of dopaminergic neurons. These neurons constitute the grey matter, in reference to their dark color caused by their high neuromelanin content (Birkmayer & Hornykiewicz, 1961; Stansley & Yamamoto, 2015). The reason why L-DOPA is suitable for therapy of Parkinson's disease is because of its ability to cross the blood-brain barrier and enter into nerve cells where it

doi:10.6342/NTU202301575

is decarboxylated to dopamine (Wade & Katzman, 1975). Exogenously supplied L-DOPA can enhance dopamine level in a Parkinson's patient's brain and replenish disappearing melanin in the brain to sooth the symptoms.

In the plant kingdom, L-DOPA was identified as an allelochemical secreted by a few species to inhibit the growth of their neighbor. Allelopathy is defined as a phenomenon including both positive and negative effects of plants or microbes on other organisms by means of chemicals, described as allelochemicals, which these species produce (Mallik, 2002). L-DOPA is found large in quantities (1% in the leaves and 4–7% in the seeds), in velvet bean (*Mucuna pruriens* (L.) *var. utilis*), a legume from the Fabaceae family with high nutritional quality nearly equal to soybean (Pugalenthi et al., 2005), and in the broad bean *Vicia faba*, a widely cultivated species in Europe and Asia.

In the L-DOPA oxidation pathway leading to the formation of melanin, L-DOPA first forms the unstable dopaquinone and dopachrome, which subsequently produces 5,6-dihydroxyindole-2-carboxylic acid (DHICA) and 5,6-dihydroxyindole (DHI). The most widespread form of melanin consists in brown to black eumelanins which are formed by copolymerization of DHI and DHICA (Ozeki et al., 1997). Animal hair color varies from light brown to black depending on the proportion of DHI and DHICA that they contain. An article by a Japanese group once pointed out that through aging, the eumelanin composition in human hair changes. With aging, the percentage of DHI rises

doi:10.6342/NTU202301575

up while the proportion of DHICA goes down. The change in DHI and DHICA ratio contributes to the hair color change of Japanese women (Itou et al., 2019).

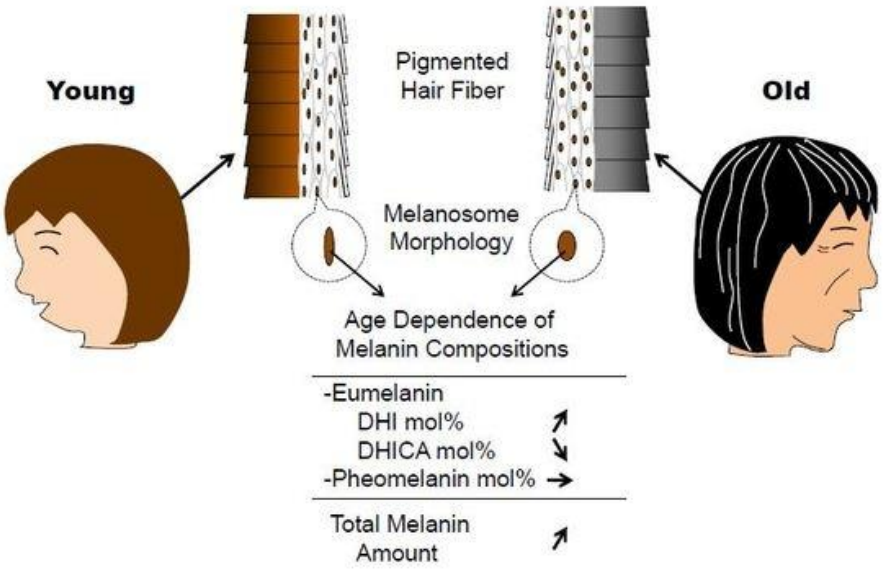

Supplementary Figure S1.6 | The human hair DHI/DHICA ratio goes up with aging. In the 2019 studies, it was pointed out that a significant positive correlation with age is found in the total melanin amount of hair and the percentage of DHI in hair eumelanin (Itou et al., 2019).

doi:10.6342/NTU202301575

1.6 L-DOPA and Fe: choosing L-DOPA as a plant Fe biostimulant

In 2011, a microarray analysis demonstrated that exogenous application of the plant allelochemical produced by legumes — L-DOPA to *Arabidopsis thaliana* led to an upregulation of Fe deficiency genes in roots. The first intention of this research is to explore the mechanism how L-DOPA inhibits plant growth, however the researchers got different results than expected. The most upregulated gene was *IRON MAN 1*(*IMA1*/At1g47400), which encodes a peptide that is necessary and sufficient to trigger Fe accumulation to very high concentration (Golisz et al., 2011b; Grillet et al., 2018).

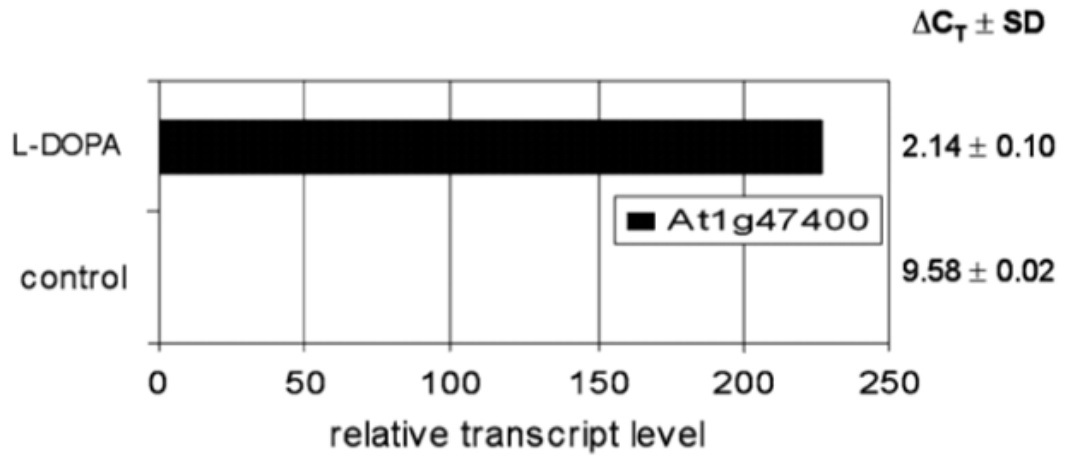

Supplementary Figure S1.7 | L-DOPA triggers the expression of *IRON MAN 1*(*IMA1*/At1g47400) gene. 6-hour, 500 μM (100 ppm) L-DOPA treatment gives rise to the huge expression level increase of *AtIMA1* (Golisz et al., 2011b).

doi:10.6342/NTU202301575

From this experiment we hypothesized that L-DOPA can mimic a Fe deficiency response by increasing the production of IMA1 peptides which subsequently serve as a dummy target for the negative regulators of Fe uptake, BTS and BTS-like E3 ubiquitin ligases. This leads to the inhibition of FIT degradation (see point 1.2.2), and therefore can enhanced expression of Fe uptake genes.

In addition, L-DOPA can behave as a Fe chelator in the human body. It was reported in 2019 that in human brains, dopamine autooxidation to neurotoxic dopamine quinones might be the root cause of Parkinson's disease pathogenesis. The rate of dopamine quinone formation increases when there is excess redox-active Fe, thereby exacerbating the severity of Parkinson’s disease. Different from dopamine, its precursor L-DOPA has the function to chelate redox-active Fe and stop dopamine from continuous autoxidation. According to this report, L-DOPA molecules can chelate Fe ions in both Fe (II) and Fe (III) forms at a 3 to 1 ratio (Billings et al., 2019).

doi:10.6342/NTU202301575

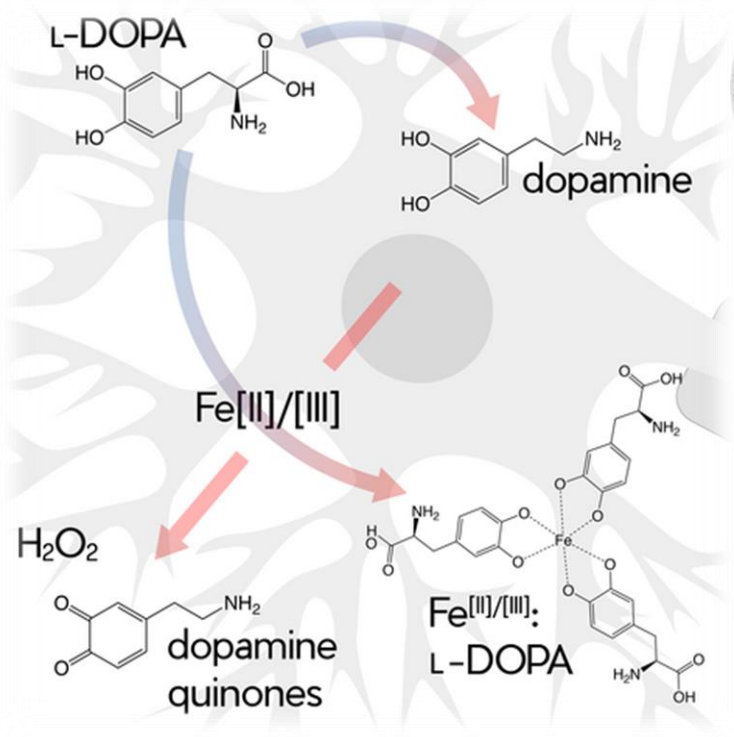

Supplementary Figure S1.8 | L-DOPA has Fe chelating properties. Based on the discovery in 2019, it is revealed that L-DOPA has Fe-chelating properties and play a role in the redox silencing of free Fe in neurons (Billings et al., 2019). L-DOPA can not only trigger Fe deficiency response in *Arabidopsis thaliana*, but can also chelate free Fe ions in human brains. These are the reasons why we decided to test L-DOPA's applicability to serve as a biostimulant of plant Fe uptake.

doi:10.6342/NTU202301575

2. Materials and Methods

2.1 Plant materials

Plant material used was *Arabidopsis thaliana* ecotype Colombia-0 (Col-0). The original seeds were acquired from Arabidopsis Biological Resource Center, ABRC. The filial seeds were propagated by ourselves.

2.2 Chemicals used

Analytical grade methanol (Echo chemical, CAS-No: 67-56-1) was used for HPLC; 37 % hydrochloric acid fuming (Supelco, EMSURE® ACS,ISO,Reag. Ph Eur) at analytical grade was used for adjusting the pH of mobile phases for HPLC; ethanol (Honeywell, CAS-No: 64-17-5) was used for seed sterilization ; Analytical grade ethyl acetate (ALPS CHEM CO., LTD) was used for DHICA synthesis; nitric acid, 69.0-70.0 % (J.T. Baker, Batch No: 0000275005); L-DOPA (Sigma, CAS-No: 53587-29-4); FerroZine (3-(2-Pyridyl)-5,6-diphenyl-1,2,4-triazine-4',4'-disulfonic acid; Sigma-Aldrich, CAS-No: 63451-29-6); BPDS (Bathophenanthrolinedisulfonic acid disodium salt hydrate; Thermo Scientific, CAS-No: 52746-49-3).

2.3 Growing and harvesting hydroponic Arabidopsis

2.3.1 Hydroponic system

The hydroponic system was described in pervious paper with slight modifications (Zeng

doi:10.6342/NTU202301575

et al., 2018). The system consisted of solid green containers (12 × 9.5 cm) with transparent lids, a floating pad made of white foam board, twelve Arabidopsis plants per box, and 400 ml nutrient solution/medium (ES media, detail ingredient) for each container (Estelle & Somerville, 1987). First, the white foam boards were trimmed to fit in the container and 12 holes were poked on each of the floating pads, and the caps of the microcentrifuge tubes were tucked into the holes, and a 0.1 cm diameter hole was drilled in each cap.

The following step was to fill caps with 0.7% ES-agar medium (0.7 g of agar in 100 mL of ES solution) and after the agar solidified in the lids, one seed was placed onto the agar using a toothpick, and the seeds germinated directly in the growth chamber. A small fork was used to poke a hole into the center of the pad. The fork enabled us to lift the floating pad with the plants to prevent the roots from sticking to the floating pad, and to minimize the exposure of the floating pad to the culture medium. The nutrient solution was changed at least twice a week.

doi:10.6342/NTU202301575

Supplementary Figure S2.1 | The Arabidopsis hydroponic system. All of the hydroponic Arabidopsis plants in the series of experiments were grown in this way.

doi:10.6342/NTU202301575

Supplementary Table S2.1 | Formula of the ES medium

Macronutrients	**Final concentration (mM)**
KH_2PO_4 (Merck, CAS-No: 7778-77-0)	2.5
KNO_3 (Merck, CAS-No: 7757-79-1)	5
$MgSO_4$ (Merck, CAS-No: 10034-99-8)	2
$Ca(NO_3)_2$ (Merck, CAS-No: 13477-34-4)	2
Micronutrients	**Final concentration (μM)**
H_3BO_3 (Merck, CAS-No: 10043-35-3)	70
$MnCl_3$ (Merck, CAS-No: 13446-34-9)	14
$CuSO_4$ (Merck, CAS-No: 7758-99-8)	0.5
$ZnSO_4$ (Merck, CAS-No: 7446-20-0)	1
Na_2MoO_4 (Sigma-Aldrich, CAS-No: 10102-40-6)	0.2
$CoCl_2$ (Sigma-Aldrich, CAS-No: 7791-13-1)	0.01
Fe-EDTA (made of $FeCl_3$ and EDTA)	50

doi:10.6342/NTU202301575

2.3.2 Sterilization and sowing of Arabidopsis seeds

A small volume of Arabidopsis seeds were placed at the bottom of a 1.5 mL microcentrifuge tube. Freshly prepared 6% unscented commercial bleach and 95% ethanol were mixed at a 1:2 ratio in a 15 mL tube and 1 mL of the solution was added to the seed-containing microcentrifuge tube. The sterilization solution was drained and replaced by 1 mL of 95% ethanol immediately, to rinse seeds. These steps were repeated for three times. Throughout the sterilization, the seeds were handled with care and unnecessary loss was avoided. In the last step, after pipetting out as much ethanol as possible, the seeds were dispersed and stick to the wall of the microcentrifuge tube. Seed were ready to use after drying. Seeds were sowed on the agar-contained-cap of the hydroponic system using a wet wooden toothpick.

2.3.3 Growth conditions

The Arabidopsis plants were grown under 16 h light / 8 h dark at 22 °C in a growth chamber with PPFD (Photosynthetic Photon Flux Density) at average 124.40 μmol*m^{-2}*s^{-1}. After every change of nutrient solution, the order of boxes was changed randomly to avoid growth heterogeneity. Two-week-old Arabidopsis seedling were transferred to condition media with L-DOPA of hydroponic system. These were different from direct germination treatments (see point 2.3.5), which received exogenous L-DOPA from the germination.

doi:10.6342/NTU202301575

2.3.4 L-DOPA dissolution

There were two ways to dissolve L-DOPA, whether in basic or in acidic conditions. The steps to dissolve L-DOPA in basic condition were as followed: L-DOPA stock solution (0.5 M) was prepared with 100 mg L-DOPA powder dissolved in 1 mL 1.3 M KOH in a 1.5 mL microcentrifuge tube. The stock solution would gradually oxidize and became brownish so it should be dissolved in nutrient solution within thirty minutes.

The steps to dissolve L-DOPA in acidic condition are as following: 10 mL 50 mM L-DOPA in HCl stock solution was prepared with 100 mg L-DOPA powder dissolved in 10 mL 0.1 N HCl in a 15 mL centrifuge tube. After L-DOPA dissolved in HCl, the color of the solution did not turn brown and remained transparent.

Fully oxidized L-DOPA in KOH was only used in the oxidized L-DOPA experiments (Paragraph 4.4; Figure 4.9 and 4.10). 10 mL 0.5 M fully oxidized L-DOPA stock solution was prepared with 1g L-DOPA powder dissolved in 10 mL 1.3M KOH in a 25 mL Erlenmeyer flask. The flask containing L-DOPA in KOH was placed on an orbital shaker, and shaken at 80 rpm and at room temperature for 3 days. After dissolution of L-DOPA in KOH the color of the solution inside the flask turned increasingly darker through hours and days. The color of the fully-oxidized DOPA in KOH ended up to be close to black.

doi:10.6342/NTU202301575

2.3.5 L-DOPA treatment conditions

L-DOPA treatments were carried out on hydroponically-grown plants (Paragraph 3.1.1 and 3.4). Plants were grown on control (ES solution, no treatment), Fe deficient (ES solution without Fe-EDTA); ES solution containing 50-500 μM L-DOPA for 5 days. The result is the mean value obtained from 3 independent boxes, and 3-4 plants among the 12 plants per box is a replicate. Each box can provide at least 3 replicates.

For the qPCR experiments (Paragraph 3.2), the following plant materials were prepared: Arabidopsis grown in – L-DOPA (control) and + L-DOPA conditions. The L-DOPA concentration used was 250 μM. The treatments lasted for 24 hours and the roots of the plants were harvested and frozen. The result is the mean value obtained from 2 independent boxes of plants. The rationale of plant replicates is the same as above.

In order to investigate the relationship between EDTA and L-DOPA (Paragraph 3.3), the following treatments were implemented: plants were treated with + Fe-EDTA – L-DOPA (control), + Fe-EDTA + L-DOPA, + $FeCl_3$ – L-DOPA and + $FeCl_3$ + L-DOPA conditions. The concentration of Fe-EDTA and $FeCl_3$ used was 50 μM and the L-DOPA concentration used was 250 μM. The treatments lasted for 3 days. The result is the mean value obtained from 2 independent boxes of plants. The rationale of plant replicates is the same as above.

For the oxidized L-DOPA experiments on hydroponically-grown plants (Paragraph

doi:10.6342/NTU202301575

4.4), the following treatments were executed: normal ES solution; ES solution containing 250 μM L-DOPA (in HCl); ES solution containing 250 μM fully oxidized L-DOPA (in KOH); Fe deficient (ES solution without Fe-EDTA but with FerroZine); Fe deficient ES solution containing 250 μM L-DOPA (in HCl); Fe deficient ES solution containing 250 μM fully oxidized L-DOPA (in KOH) for 3 days. The result is the mean value obtained from 3 independent boxes of plants. The rationale of plant replicates is the same as above.

For the melanin precursors (L-DOPA, DHI, DHICA) and HICA (5-Hydroxyindole-2-carboxylic acid) experiment (Paragraph 4.3), the following treatments were executed: First, DHI, DHICA and HICA were dissolved in a small volume of DMSO. Afterwards, the stock solution of DHI, DHICA and HICA were added into the ES hydroponic medium and the final concentration for them are 250 μM. The L-DOPA treatment was carried out as detailed above also at the final concentration of 250 μM. Measurements were performed after 3 days of treatment, on 2 independent sets of plants. The rationale of plant replicates is the same as above.

2.3.6 Direct germination of Arabidopsis in hydroponic system

Arabodopsis seeds were sown on ES agar medium, embedded in the pads floating on ES nutrient solution containing a range of L-DOPA concentrations.

doi:10.6342/NTU202301575

For the high concentration range of L-DOPA (Paragraph 3.1.2), the plants were subjected to the following treatments: Control (ES solution, no treatment); Fe deficiency (ES solution without Fe-EDTA); ES solution containing 50, 100, 250, and 500 μM L-DOPA. The nutrient solution was replaced every 3 days and the plants were grown for 14 days. Measurements were performed on two independent sets of plants. The rationale of plant replicates is the same as described in 2.3.5.

For the low concentration range of L-DOPA (Paragraph 3.1.2 and 3.4), plants were subjected to the following treatments: Control (ES solution no treatment); Fe deficiency (ES solution without Fe-EDTA and with FerroZine); ES solution containing 5, 10, 25 and 50 μM L-DOPA. The nutrient solutions were renewed every 3 days and the plants were grown for 14 days. Measurements were performed on 2 independent sets of plants. The rationale of plant replicates is the same as described in 2.3.5.

2.3.7 Ferric-chelate reductase (FCR) assay

After treatments, roots of hydroponically-grown plants were harvested and washed in 5 mM MES buffer, pH5.5. Then the roots of each plant were subjected to FCR assay. The assay solution consisted in 2 mL of 5 mM MES, pH5.5, 300 μM bathophenanthroline disulfonic acid (BPDS) and 100 μM Fe(III)-EDTA. Roots of plants subjected to different treatments were immersed in 2 mL assay solution in a 24-well

doi:10.6342/NTU202301575

plate. The plate was kept in dark and placed on an orbital shaker for 1 hour, shaking at 80 rpm. 200 μL assay solution were transferred into a spectrophotometer 96-well plate, and the absorbance at 535 nm was measured using a plate spectrophotometer (TECAN, Infinite® 200 PRO). Roots were subsequently dried with paper towels carefully, in order to avoid to overly dehydrate them. Roots fresh weight (FW) were measured using a precision balance. After collecting the absorbance and root weight data, the FCR activities in μmol Fe^{II} per hour and per gram of roots were calculated by the following steps:

- A standard curve was needed. First was to prepare standard solutions. $FeSO_4$ concentrations of the standards were 0, 2.5, 5, 10, 25, 50, 75 and 100 μM. According to the standard concentrations, different quantities of $FeSO_4$ solution were pipetted to the 96-well plate, and then 200 μM MES buffer containing 300 μM BPDS was added to $FeSO_4$ containing wells. OD_{535nm} of the standard solutions were measured.
- OD_{535nm} on the $FeSO_4$ standard concentrations were plotted. A trendline and its equation were displayed on the chart. This was the standard curve.
- the equation was used to calculate $[Fe^{II}\text{-}BPDS_3]_{sample}$ from the measured OD_{535nm}.
- From the concentrations acquired in last step, the amounts of μmole of $Fe^{II}\text{-}BPDS_3$ formed during the root FCR reactions were calculated (reaction volume = 2 mL).

doi:10.6342/NTU202301575

2.4 Arabidopsis cultivation on soil

2.4.1 Soil, pots, and watering

The soil was a mix of perlite vermiculite, and potting soil (Jiffy Group, Netherlands) with 1:1:4 ratio. Pots (with 7.62 cm diameter) were filled with the soil mixture. Soil in the pots was pressed a little to be compact flattened then put into a plastic platter. The soil was irrigated with Reverse Osmosis (R.O.) water thoroughly. After sowing Arabidopsis seeds on the soil, the plants should be irrigated at least once a week with about 100 mL RO water per pot; after bolting, the soil should be watered twice a week; after the siliques of plants reached maturing stage, watering should be stopped.

2.4.2 Sowing seeds onto the soil

A weighing paper was taken and loaded with 10-15 Arabidopsis seeds. Seeds were sown in a wet-soil-filled pot homogenously by dithering the seed-loaded weight paper everywhere on the pot. After sowing, the plastic platter filled with pots was covered by a transparent plastic dome to maintain the humidity of the inner space. The dome could be removed after 2 weeks, when the Arabidopsis plants reached the 4-leafed stage; by then, extra plants were removed and one plant was left in each pot.

doi:10.6342/NTU202301575

2.4.3 Plant Growth conditions

The Arabidopsis plants were grown under 16 h light / 8 h dark at 22 °C with an average PPFD of 124.40 μmol*m^{-2}*s^{-1}. After the Arabidopsis bolted, a plastic tutor was thrusted into the middle of the pot. The floral stems of Arabidopsis were tied to the stick to guide them to grow upwards.

2.4.4 L-DOPA treatment

L-DOPA stock solution (0.5 M) was prepared with 100 mg L-DOPA powder dissolved in 1 mL 1.3M KOH in a 1.5 mL microcentrifuge tube. The stock solution gradually oxidized and became brown. It was therefore used within a half hour.

The L-DOPA treatments on soil were performed as followed: water the plant with 100 mL RO water containing 0, 50, 250, 1000, 3000 μM L-DOPA. Each treatment was carried out on 9 individual plants.

2.5 Fe quantification

Fe in rosettes and seeds of Arabidopsis were quantified by spectrophotometry. The standard curve of Fe quantification was prepared with a range of Fe concentrations: 0, 1.25, 2.5, 5, 10, 20, and 40 μg of Fe in glass test tubes, corresponding to 0, 0.45, 0.9, 1.79, 3.58, 7.17, and 14.34 μL of 50 mM Fe-EDTA dissolved in water.

For Fe quantification in Arabidopsis rosettes, 3 week-old rosettes were harvested

doi:10.6342/NTU202301575

and washed with RO water to remove nutrient solution or soil residues, and placed in 50 mL centrifuge tubes and dried at 60°C oven overnight. About 15 mg of dry leaf tissues of each treatment was transferred into a glass test tube.

For seed Fe quantification, around 5 mg of seeds were taken out and transferred into a glass test tube.

The remaining steps of rosette and seed Fe quantifications were identical. 225 µL of 65% (v/v) nitric acid (HNO_3) was added to each sample containing tube carefully, to avoid pipetting any drop of HNO_3 on the tube wall. The whole process was carried out inside a fumehood. The tubes were subsequently placed into a heatblock and heated at 96°C until the samples completely dissolved in HNO_3. 150 µL of H_2O_2 was added to each tube and the tubes were later placed into the heatblock again and heated at 56°C. After H_2O_2 discolored the liquid inside the tubes, 225 µL of ultra-pure water was added to each tube. We used BPDS solution to perform the colorimetric tests. BPDS solution consisted of RO water, 1 mM BPDS, 0.6 M sodium acetate, 0.48 M hydroxylamine and was freshly prepared after the sample digestion. 235 µL of BPDS solution was mixed with 15 µL of digested sample in a spectrophotometer 96 well-plate and the absorbance at 535 nm of each sample was measured using a plate spectrophotometer (TECAN, Infinite® 200 PRO). The absorbance of each sample was recorded. The method to prepare the standard curve was identical to Paragraph 2.3.7. Fe concentrations in

doi:10.6342/NTU202301575

rosettes were calculated by Excel.

2.6 Synthesis of DHICA

The procedure of DHICA synthesis was as described in Charkoudian and Franz, 2006 with minor modifications (Charkoudian & Franz, 2006). DHICA was prepared under inert condition with a pump and an Erlenmeyer flask, creating a vacuum environment (Figure 2.2). 0.5 g L-DOPA powder was first dissolved in 250 mL RO water in a flask. A solution of $K_3[Fe(CN)_6]$ (3.3g, 20 mM) and $NaHCO_3$(1.25 g, 30 mM) in 30 mL H_2O was added over the course of 3-5 min into the stirred solution of the 5 mM L-DOPA solution. The L-DOPA solution became wine-red after $K_3[Fe(CN)_6]$ and $NaHCO_3$ were added. 35 mL of 1 M NaOH at pH 13 was added into the flask. After 15 minutes of stirring, the reaction mixture was quenched with 8 mL of 6 M HCl. The pH was then adjusted to 2 with HCl. The reaction mixture was then extracted with 3 × 125 mL of ethyl acetate with a lap funnel. The combined ethyl acetate extract was washed with 50 mL saturated NaCl solution containing 10 mM $Na_2S_2O_4$, afterwards, the extract was then washed another 2 times by 50 mL saturated NaCl solution. The extract was finally dried with Na_2SO_4. Remained ethyl acetate was evaporated using a rotary evaporator (Figure 2.3). Evaporation gave a pale brown solid, which was dissolved in 12.5 mL acetone. The addition of 100 mL hexane produced a brown oil, which was

doi:10.6342/NTU202301575

discarded. An additional 75 mL of hexane was added, leading to the crystallization of DHICA as a white powder. The identity and purity o DHICA was verified by LC-MS-MS. The rotary evaporator was kindly borrowed from Prof. Lean-Teik Ng (Department of Agricultural Chemistry, National Taiwan University).

Figure 2.2 | The homemade vacuum system for DHICA synthesis. The pump sucked out the air to maintain an environment under vacuum inside the flask, because oxygen would interfere with the DHICA synthesis process. The reagents was added into the flask using syringes by inserting the needle through the rubber stop of the flask. The solution was continuously mixed using a magnetic stirrer.

doi:10.6342/NTU202301575

Figure 2.3 | A rotary evaporator was used to evaporate the solvent. The DHICA ethyl acetate mixture was in the larger balloon inside the water bath. The boiling points of ethyl acetate reduced on decreasing pressure of the rotary evaporator, thus ethyl acetate vaporized at a much lower temperature than its boiling point at normal pressure. After being cooling down, the hexane condensed back to liquid status and was collected in the smaller balloon, leaving dry DHICA on the wall of the larger balloon.

doi:10.6342/NTU202301575

2.7 Analytical procedures

2.7.1 High-performance liquid chromatography (HPLC)

The detection of L-DOPA, DHI, DHICA was conducted on a Hitachi HPLC D-2000 system, composed of a L-2455 diode array detector, a L-2200 autosampler, and a L-2130 pump. A reverse phase C_{18} column, Cosmosil 5C_{18}-AR-II (4.6 × 250 mm, 5 μm, Waters, Milford, MA, USA), was used at 30 °C. The mobile phase used was made of 100% solvent A (1:3 methanol/water solution acidified with hydrochloric acid, pH 2.5). The injection volume was 10 μL per sample and the detection wavelength was monitored at 282 nm for L-DOPA; 300 nm for DHI and DHICA. The settings of gradient and flow rate were shown in Supplementary Table S2.2. The HPLC instrument was kindly borrowed from Prof. Pei-Jen Chen (Department of Agricultural Chemistry, National Taiwan University)

Supplementary Table S2.2 | Settings of gradient and flow rate on HPLC

Time (min)	A (%)	Flow (mL/min)
0	100	1.0
10	100	1.0

A: 1:3 methanol/water solution acidified with hydrochloric acid, pH 2.5

doi:10.6342/NTU202301575

2.7.2 Liquid chromatography-tandem mass spectrometry (LC-MS/MS)

The LC-MS/MS was performed by Yu-Ching Wu from the Metabolomics Core Facility of the Agricultural Biotechnology Research Center of Academia Sinica. The chromatography was performed using a BEH phenyl column (2.1 mm × 100 mm, 1.7 μm, Cat # 186002885) at 40 °C with a mobile phase consisting of solvent A (2 % ACN/98 % H_2O + 0.1% formic acid) and solvent B (100 % ACN + 0.1 % formic acid). The injection volume was 5 μL. The settings of gradient and flow rate were shown as following.

Supplementary Table S2.3 | Settings of gradient and flow rate on LC-MS/MS

Time (min)	A (%)	B (%)	Flow (mL/min)	Curve
0	99.5	0.5	0.4	6
4.0	0.5	99.5	0.4	6
5.0	0.5	99.5	0.4	6
5.1	99.5	0.5	0.4	6
6.0	99.5	0.5	0.4	6

A: 2 % ACN/98 % H_2O + 0.1% formic acid

B: 100 % ACN + 0.1 % formic acid

General instrumental conditions were sheath gas, auxiliary gas, and sweep gas of

doi:10.6342/NTU202301575

35, 15, and 1 arbitrary unit, respectively. Ion transfer tube temperature was 360 °C; vaporizer temperature was 350 °C; spray voltage was 3200 V in positive mode. For analysis, a full MS scan mode was set with a m/z scan range from 70 to 1000 and resolution 15000 was applied. The Xcalibur 4.1 software (Thermo Scientific) was used for data processing.

2.8 Gene expression analysis

2.8.1 RNA extraction from roots

Arabidopsis root samples were frozen in liquid nitrogen and stored at -80°C. The roots were collected into 2 mL pre-labeled microcentrifuge tubes (QSP Cat. #508-GRD-Q) containing a stainless-steel bead (Cat. #SB1606-4) inside. The roots were ground using pre-cooled bead mill (LAWSON scientific), kindly borrowed from Professor Chwan-Yang Hong. The total RNA was extracted from the root powder using RNeasy Mini Kit (Qiagen). The extraction was performed following the instruction manual.

2.8.2 cDNA synthesis

One μg of total RNA per sample was used as a template to synthesize cDNAs. TOOLSQuant RT kit was used for first-strand cDNA synthesis (BIOTOOLS, Cat. No. TGKRA03). The Reverse Transcription reaction was performed according to the instruction manual.

doi:10.6342/NTU202301575

2.8.3 qPCR

The resulting single-stranded cDNAs were then used as a template for Real-Time Quantitative Polymerase Chain Reacion (RT-qPCR). RT-qPCRs were carried out with gene-specific primers listed in Supplementary Table S2.4, and SYBR™ Green PCR Master Mix (Applied Biosystems, Cat. No. 4309155) according to the manufacturer's instructions, using a QuantStudio 12K Flex Real-Time PCR System. Three independent replicates were measured for each sample. The ΔΔCT method was used to determine the relative gene expression (Livak & Schmittgen, 2001), with the expression of elongation factor 1 alpha (EF1α; At5g60390) used as an internal control.

Supplementary Table S2.4 | Primers used for qPCR

Primer name	sequence
q*AtEF1α* Fp	GAGCCCAAGTTTTTGAAGA
q*AtEF1α* Rp	CTAACAGCGAAACGTCCCA
q*AtFRO2* Fp	GATCGAAAAAAGCAATAACGGTGGTT
q*AtFRO2* Rp	GATGTGGCAACCACTTGGTTCGATA
q*AtIRT1* Fp	CGTGCGTCAACAAAGCTAAA
q*AtIRT1* Rp	TCTGGTTGGAGGAACGAAAC

doi:10.6342/NTU202301575

2.9 Anthocyanin extraction and quantification

2.9.1 Sample processing

2 mL pre-labeled microcentrifuge tubes (QSP Cat. #508-GRD-Q) with a stainless-steel bead (Cat. #SB1606-4) inside were weighed. After placing about one to two fresh rosettes into each tube, the tubes were frozen immediately at -80 °C. The rosettes were then freeze-dried with a freeze-drier (KINGMECH) overnight. The tubes containing the dry samples were weighed. The weight of the dry samples could be calculated by subtracting the weight of the tube with the bead. The dry samples were ground into fine powder using bead mill (LAWSON scientific) at the frequency of 42 Hz for 15 seconds twice with a 10 second gap in between. The bead mill was kindly borrowed from Professor Chwan-Yang Hong.

2.9.2 Anthocyanin extraction

400 μL methanol was added to each tube and incubated for 15 minutes with shaking at 1500 rpm. Afterwards, 200 μL chloroform was added to the tubes with shaking for 5 minutes at the same speed. Finally, 400 μL RO water was added and the tubes were vortexed vigorously for 1 minute. The tubes were then centrifuged at 15,000 g for 10 minutes. 400 μL of supernatant from each tube was transferred to a new, pre-labeled tube. 100 μL of 0.3 M HCl was added to each tube to reveal the pink color of

doi:10.6342/NTU202301575

anthocyanins. Absorbance at 532 nm were measured. The anthocyanin concentration was shown in the form of absorbance unit per gram of dry tissues. There is no standard for anthocyanin in this method.

2.10 Fe-driven L-DOPA oxidation kinetics measurement

2 μL 0.25 M L-DOPA and 2 μL 50 mM Fe source (Fe-EDTA/$FeCl_3$) were dropped on different side of the wall of a 3.5 mL10 mm quartz cuvette. 20 μL of 30 mM BPDS was directly put in the bottom of the cuvette. The spectrophotometer program—kinetic measurement was set with the observed wavelength at 535 nm. Another cuvette with 2 mL RO water was inserted into the groove for blank. The machine was firstly blanked, and the cuvette with sample was inserted in the groove for sample. 2 mL of RO water was flushed into the sample-contained cuvette at the last second and the lid of the spectrophotometer was shut. Absorbance changes were measured. Every 10 seconds a data point was required. The data acquisition process lasted for 10 minutes. The kinetics curve of L-DOPA oxidation in Fe-containing solution was made using Excel. The experiment was performed 3 times. The SHIMADZU UV-1900i spectrophotometer was kindly borrowed from Professor Hsi-Mei Lai.

doi:10.6342/NTU202301575

2.11 Statistical analysis

Bar charts were drawn according to the raw data using Excel. Statistical tests were executed using R 4.2.2 and Excel. The grouping method used after ANOVA was Fisher's LSD (Least Significant Difference) with the P-value threshold set at 0.05. The statistical hypothesis test used was Student's t-test.

doi:10.6342/NTU202301575

3. Results—Part I

In part I, we applied L-DOPA to both hydroponic and soil-grown experiments. For the hydroponics, we treated the plants for one or three weeks, depending on the L-DOPA concentrations used in the hydroponic solution. The L-DOPA concentrations used in soil-grown experiment are much higher than hydroponics because soil has a strong buffering and diluting capacity.

The aim of part I was to see whether L-DOPA can trigger plant Fe deficiency response and boost Fe content inside a plant and its seeds.

3.1 L-DOPA increased Arabidopsis Fe uptake in hydroponics

3.1.1 L-DOPA enhanced FCR activity of Arabidopsis roots but arrests plant growth at high concentrations

As we know from the introduction, L-DOPA has been suggested to deregulate metal homeostasis especially Fe in Arabidopsis in a previous study (Golisz et al., 2011a). The Ferric Reduction oxidase (FRO) is a reductase responsible for transforming Fe (III) into Fe (II) at the root surface, in order to support the ferrous Fe uptake by dicot plants, thus we deduce that the activity of Arabidopsis root FCR (in this case AtFRO2, Ferric Reduction Oxidase 2) might be influenced by L-DOPA addition to growth

doi:10.6342/NTU202301575

medium. We observed that roots of hydroponic Arabidopsis treated with L-DOPA had higher FCR activity compared to untreated plants (Figure 3.1), the result supports our hypothesis. L-DOPA has the ability to stimulate root Fe uptake. The higher L-DOPA concentration in the hydroponic medium, the higher root FCR activity we measured. However, we also observe that L-DOPA inhibited plant growth at concentrations higher than 50 μM (Fig. 3.2).

doi:10.6342/NTU202301575

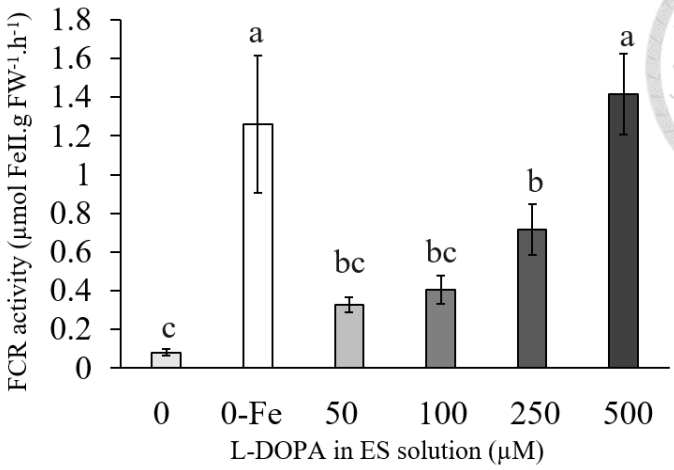

Figure 3.1 | Root FCR activity of transferred Arabidopsis plants with a range of L-DOPA concentrations in hydroponic system. Fourteen-day-old wild type (Col-0) Arabidopsis plants are treated with L-DOPA at concentration 0 (±Fe), 50, 100, 250, and 500 μM for another 7 days. Treatments other than 0 μM only consisted of normal ES recipe plus different concentrations of L-DOPA. The results were the mean values obtained from 3 independent boxes, 3-4 plants among the 12 plants per box is a replicate. Error bars stand for standard errors; the multiple comparison method used is Fisher's LSD (p-value < 0.05). Confidence intervals for all pairwise differences between factor levels are indicated by different letters.

The leaves of L-DOPA treated plants were obviously darker and smaller than those of controls (Fig. 3.2). These results suggest that anthocyanin may accumulate in leaves under L-DOPA condition. Overall, the results show that L-DOPA arrests plant growth

doi:10.6342/NTU202301575

because of its allelopathic nature, but it can boost the capacity of a plant to reduce more Fe from the environment.

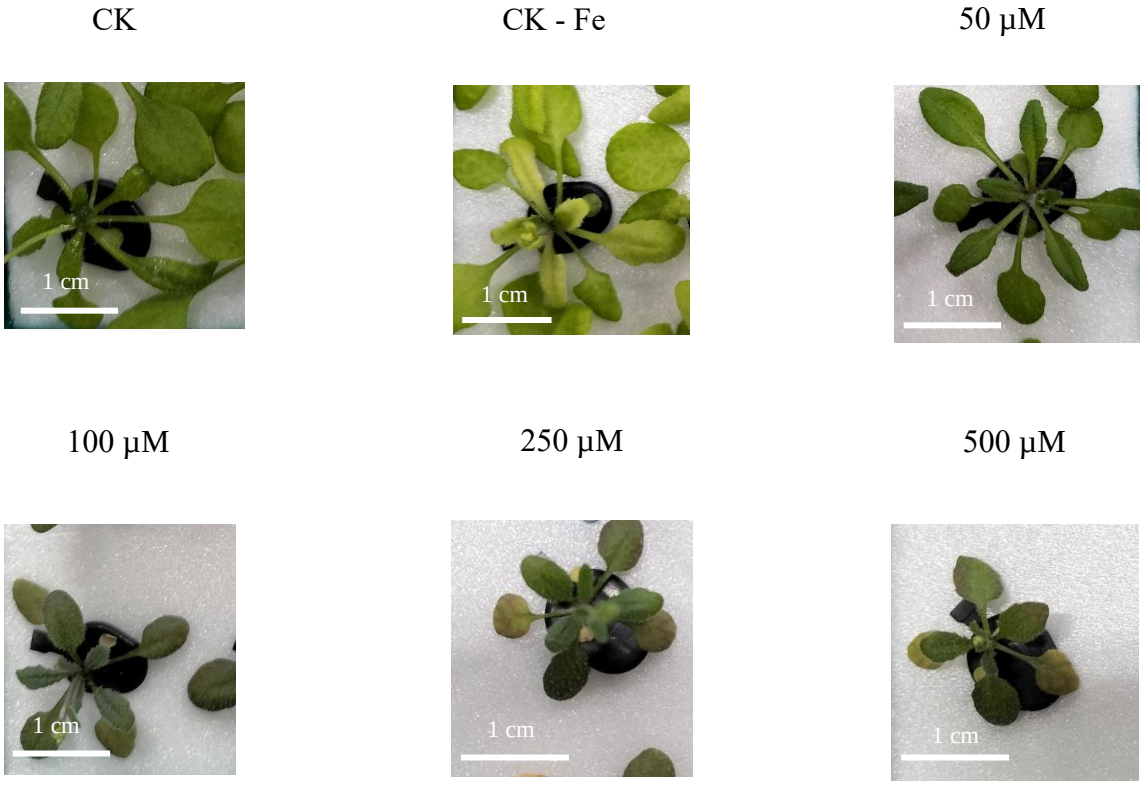

Figure 3.2 | Hydroponically-grown Arabidopsis treated with series concentrations of L-DOPA for one week. These are the pictures of the Arabidopsis plants grown for 14 days in ES medium and subjected to different concentrations (50, 100, 250, 500 µM) of L-DOPA treatments for another 7 days. CK, control (normal ES medium); CK - Fe, control minus Fe. Scale bar = 1 cm.

doi:10.6342/NTU202301575

3.1.2 The allelopathic properties of L-DOPA did not cause the plant growth inhibition at low concentration in hydroponics system

Arabidopsis seeds were directly sowed in the hydroponic system containing the range of L-DOPA (0, 50, 100, 250 and 500 μM). We find out that the conditions were too harsh for seedlings to thrive, despite the fact that they still did germinate (Fig. 3.3). Based on the observation, we reduce the L-DOPA concentration applied to the ES medium for direct germination to 0, 5, 10, 25 and 50 μM and grow them for 3 weeks. The size of rosettes was almost the same as control after 3 weeks, except 50 μM L-DOPA treated plants, which has smaller and darker leaves. However, the 50 μM L-DOPA treated plants could still grow (Fig. 3.4). This result showed that 50 μM L-DOPA was critical for L-DOPA to fully reach its allelopathic potential. From the FCR assay of 3-week L-DOPA treated plants, we observe that as long as L-DOPA is added to the growth medium, no matter how low the concentration is, the Fe uptake capacity of plant roots can be enhanced (Fig. 3.5).

The two figures of FCR assay acquired from 1 week L-DOPA treatments and 3-week L-DOPA treatments show that the effects of L-DOPA are similar on increasing root Fe uptake capacity. It means that plants treated with higher concentrations of L-DOPA but with shorter treatment time has similar, or slightly better FCR boosting

doi:10.6342/NTU202301575

effect than plants treated with lower concentrations of L-DOPA throughout their lifetime.

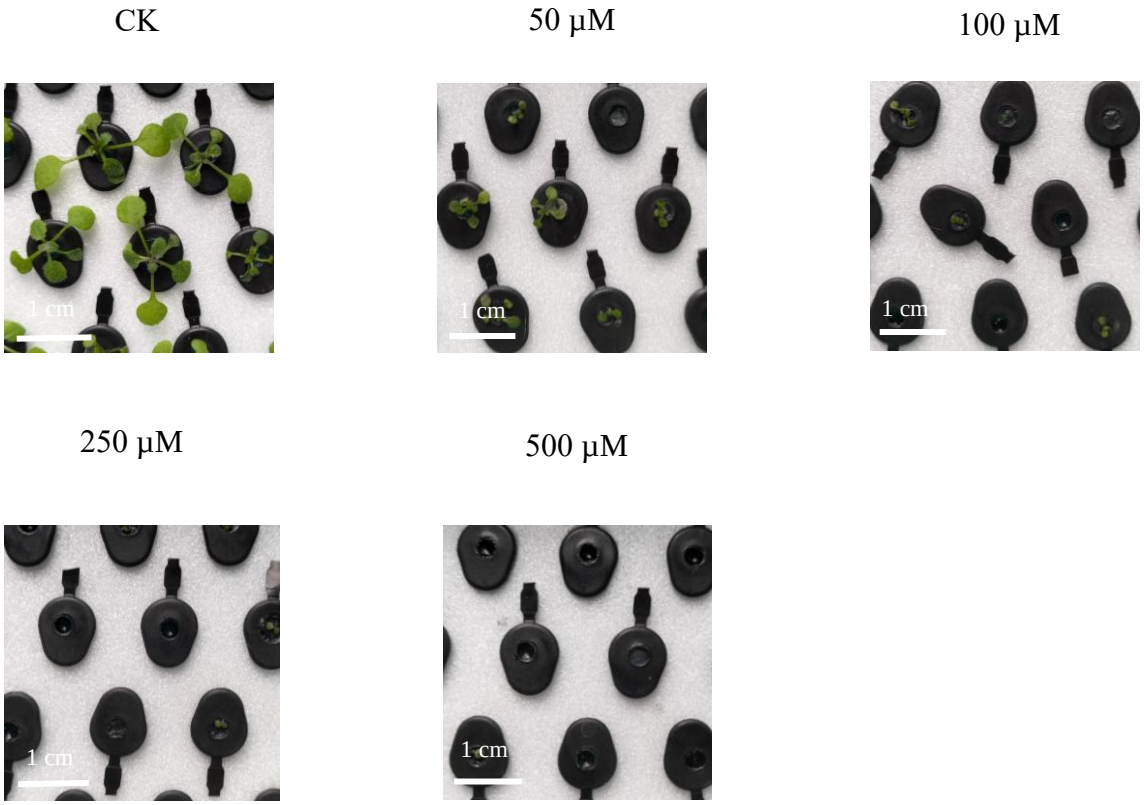

Figure 3.3 | Directly germinated hydroponic Arabidopsis plants treated with L-DOPA for 2 weeks. This are the pictures of Arabidopsis plants directly grown for 14 days in different concentrations (50, 100, 250, 500 µM) of L-DOPA containing medium. CK, control (normal ES medium). Scale bar = 1 cm.

doi:10.6342/NTU202301575

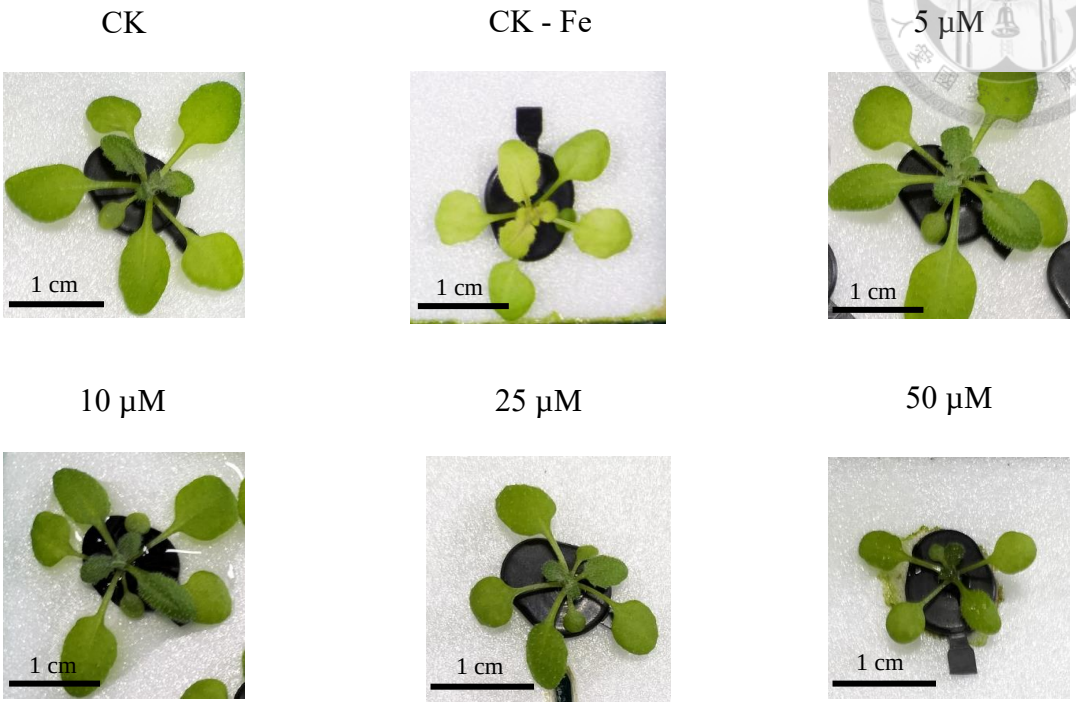

Figure 3.4 | Directly germinated Arabidopsis grown for 3 weeks under low range of L-DOPA concentrations. The pictures were taken after 3 weeks of plant directly grown in low concentration range of L-DOPA (5, 10, 25, 50 μM) containing ES medium. CK, control (normal ES medium); CK - Fe, control minus Fe. Scale bar = 1 cm.

doi:10.6342/NTU202301575

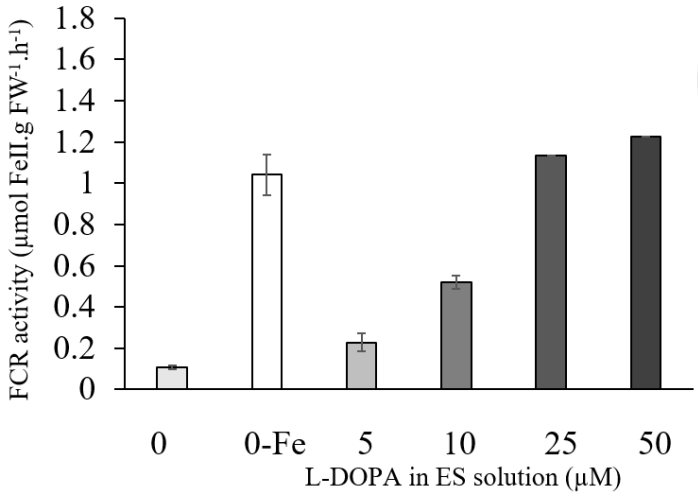

Figure 3.5 | Root FCR activity of directly germinated Arabidopsis plants under low L-DOPA concentrations in hydroponic system. 3-week-old wild type (Col-0) Arabidopsis plants are treated with L-DOPA at concentration 0 (±Fe), 5, 10, 25, and 50 μM for whole of their lifetime. Treatments other than 0 μM only consisted of normal ES recipe plus different concentrations of L-DOPA. Error bars correspond to standard error. ANOVA and following LSD were not performed in this experiment due to shortage of samples for 25 and 50 μM L-DOPA treatments. The root sample amount collected for these 2 treatments were only enough for one replicate respectively. We determined the transfer strategy was the best for boosting Arabidopsis Fe uptake from the Fe quantification results (point 3.4), so we didn't redo this specific FCR experiment.

doi:10.6342/NTU202301575

3.2 qPCRs confirm L-DOPA effect on Fe uptake capacity of Arabidopsis roots

The expression of Arabidopsis root Fe uptake genes *AtIRT1(Iron Regulated Transporter 1)* and *AtFRO2* were measured by RT-qPCR. We double-confirmed that L-DOPA can indeed boost the Fe uptake capacity of Arabidopsis.

AtIRT1 was highly induced after 24 hr treatment of 250 μM L-DOPA. The IRT1 expression level was nearly 15-fold increase in root compared to control. L-DOPA also triggered the expression of *AtFRO2*. AtFRO2 expression was increased by 8-fold after 24 hours of treatment, as compared to untreated plants. These facts were consistent with previously published data as well as our root FCR assays.

doi:10.6342/NTU202301575

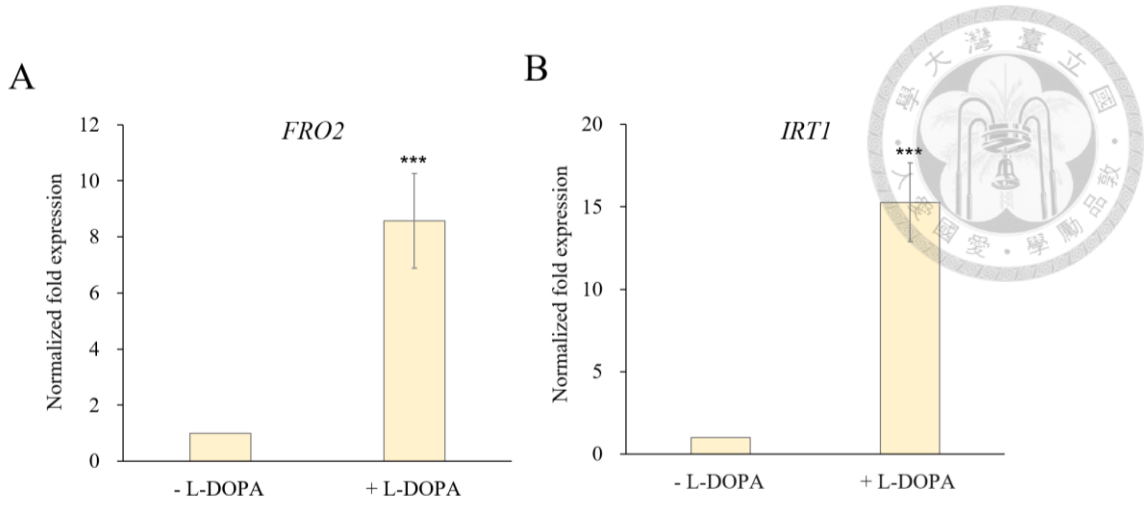

Figure 3.6 | Expression of *AtIRT1* and *AtFRO2* under ± L-DOPA treatments.

qPCR result of (A) *AtFRO2* (B) *AtIRT1* after 250 μM L-DOPA treatment for 24 hr. Result are the mean values obtained from 2 independent boxes of plants, and 3-4 plants among the 12 plants per box is a replicate for RNA extraction. RT-qPCR is measured in triplicate. Normalized fold expression was calculated by setting the expression of control (+ Fe - DOPA) as 1. "*", p-value<0.05; "**", p-value<0.01; "***", p<0.001.

doi:10.6342/NTU202301575

3.3 Interactions between L-DOPA and EDTA

3.3.1 L-DOPA synergistically acts with EDTA for stimulating plant Fe uptake

To investigate the relationship between EDTA and L-DOPA, the following experiment was performed. Two different Fe sources, Fe-EDTA and $FeCl_3$, were supplied in the ES medium of hydroponically-grown plants. Fe (III) of $FeCl_3$ is very sensitive to environment and can be reduced fairly easily by light or any reductant. The reduced Fe (II) precipitates at the bottom of the hydroponic box so the plants can hardly acquire it. Therefore, plants growing in absence of EDTA (i.e. ± L-DOPA - EDTA) are likely Fe deficient. Consistent with this hypothesis, we observed in the FCR assay that the Fe deficiency response of ± L-DOPA – EDTA plants is highly induced. In contrast, the addition of EDTA, which is a very stable Fe chelator and can prevent Fe from precipitation, allows the plants to efficiently take up Fe. In – L-DOPA + EDTA conditions, nearly no Fe deficiency response of the roots is induced, suggesting that the Fe nutrition of the plant is well supported by this medium. The – L-DOPA + EDTA-treated plants are considered as Fe-replete, and therefore have the weakest Fe deficient response. Interestingly, when the medium was supplemented with 250 μM L-DOPA (+ L-DOPA + EDTA) for 3 days, the root FCR activity increase, although it was lower than the activity measured from Fe deficient (– EDTA) plants. The results show that L-

doi:10.6342/NTU202301575

DOPA and EDTA are synergistic in affecting plant Fe uptake. If L-DOPA is present in the hydroponic normal ES medium, it can act with EDTA and make the Fe uptake ability stronger under Fe sufficient condition.

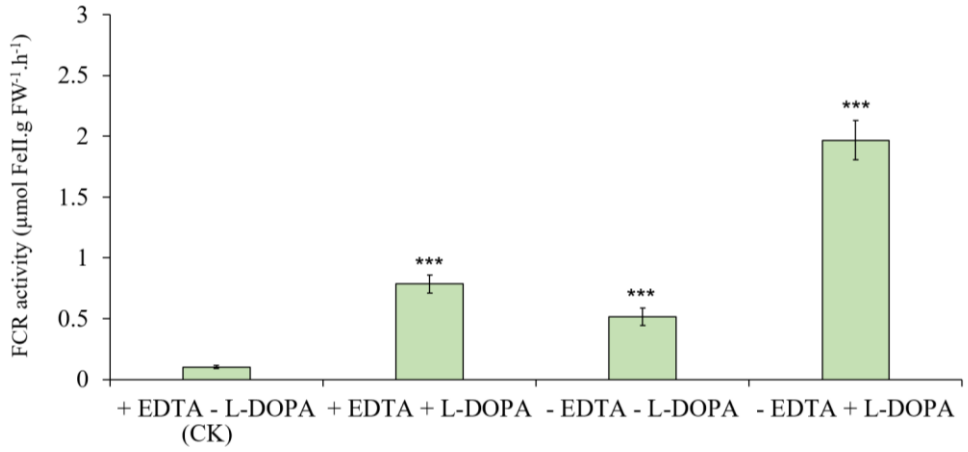

Figure 3.7 | Root FCR activities under ± EDTA ± L-DOPA treatments

Results are means of 2 independent boxes of plants with 3-4 plants per box to be a replicate. There are 6 replicates in total. CK, control (normal ES medium); + EDTA + L-DOPA, control plus 250 μM L-DOPA; – EDTA – L-DOPA, control without EDTA (only $FeCl_3$ in the ES medium); – EDTA + L-DOPA, control without EDTA (only $FeCl_3$ in the ES medium) plus L-DOPA. Error bars correspond to standard error. The statistical test used is two-tailed Student's t-test. "*", p-value<0.05; "**", p-value<0.01; "***", p<0.001.

doi:10.6342/NTU202301575

3.3.2 L-DOPA reduces free Fe (III) and gets oxidized

By studying L-DOPA oxidation kinetics, we discovered the L-DOPA oxidation patterns are different depending on the Fe sources. When Fe-EDTA is the Fe source, Fe is bound to EDTA and can't react with L-DOPA freely. Therefore, nearly no Fe (II) can be detected through time course when Fe-EDTA serves as the Fe source. On contrary, if $FeCl_3$ is the Fe source, L-DOPA can react with the free Fe (III), be oxidized into melanin and precipitate. This observation echoes over point 3.3.1, EDTA keeps Fe soluble and prevent Fe from oxidizing L-DOPA, while L-DOPA maintains high Fe uptake of a plant in the presence of EDTA.

doi:10.6342/NTU202301575

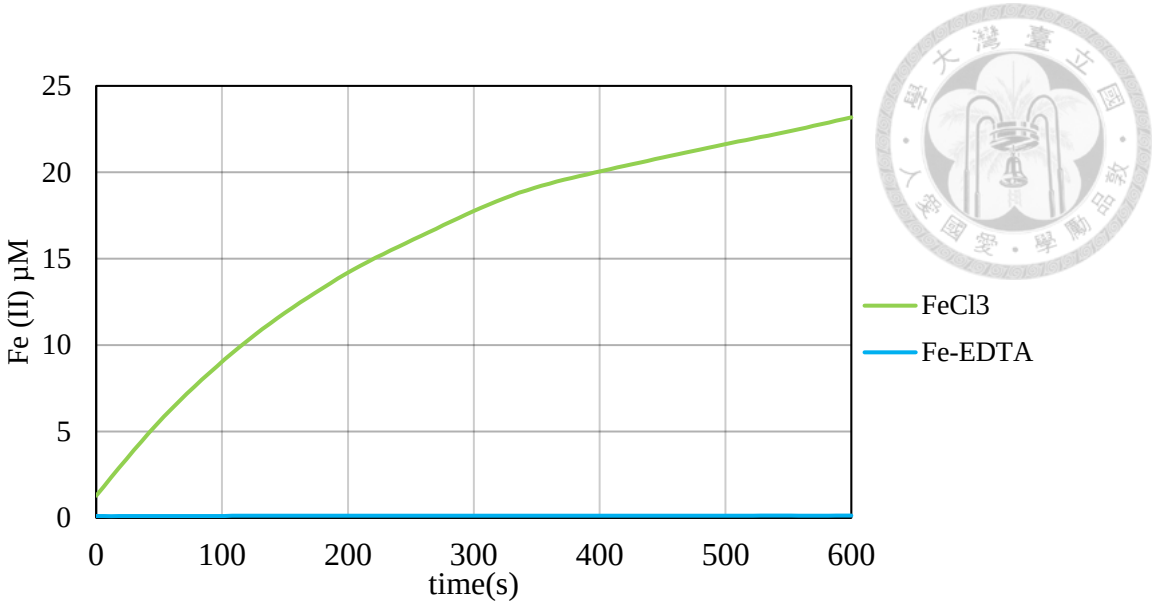

Figure 3.8 | L-DOPA oxidation kinetics by reaction with different Fe sources.

When Fe-EDTA is the Fe source for the kinetic experiment (blue line at the bottom), L-DOPA does not react with the EDTA-bound Fe (III) so no Fe(III) reduction takes place. When $FeCl_3$ is Fe source for the kinetic experiment (green curve above), L-DOPA can react with free Fe (III) of $FeCl_3$ thus reducing the free Fe (III) and becomes oxidized.

doi:10.6342/NTU202301575

3.4 L-DOPA application increases Fe concentration in Arabidopsis rosette

Fe concentrations of hydroponically-grown Arabidopsis rosettes were measured, for both plant groups treated with L-DOPA for 1 week (Fig. 3.9) and 3 weeks (Fig. 3.10).

In FCR assay, plants exposed to 500 μM exogenous L-DOPA had the highest root FCR activity, but surprisingly, the concentration of these plants was not the highest. As discussed in paragraph 3.1, L-DOPA can trigger Fe deficiency response so the more L-DOPA concentration in the hydroponic system, the stronger the capacity of roots to reduce Fe (III) to Fe (II), but it seems that this did not result in more Fe in rosettes. In summary, the ideal working concentration of L-DOPA in a hydroponic system is lower than 500 μM. Figure 3.9 shows that at 50 or 100 μM L-DOPA concentration, the Fe concentration in rosettes is the highest among all the other treatments.

In plants germinated and grown for 3 weeks on L-DOPA-containing medium, there was no obvious pattern of L-DOPA boosting rosette Fe concentration. In plants treated with L-DOPA concentrations below 50 μM, the Fe concentrations in rosettes were not significantly differ from that of control plants.

doi:10.6342/NTU202301575

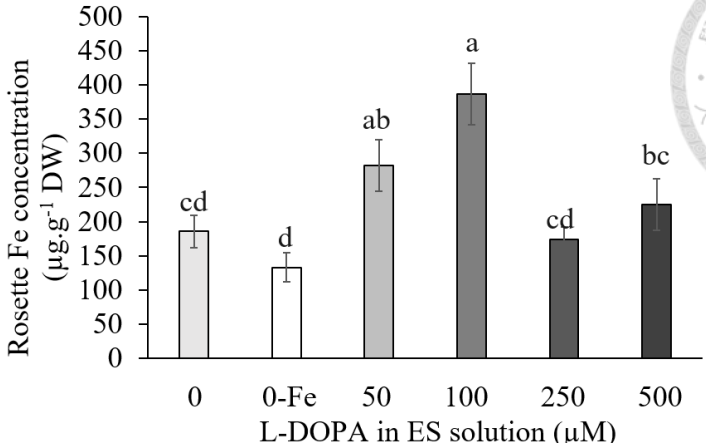

Figure 3.9 | Rosette Fe concentration of plants treated with L-DOPA for 1 week.

Fourteen-day-old wild type (Col-0) Arabidopsis plants are treated with L-DOPA at concentration 0 (±Fe), 50 (+Fe), 100 (+Fe), 250 (+Fe), and 500 (+Fe) µM for another 7 days. Results are means of 3 replicates, each replicate consists of 3-4 dry plants. Error bars correspond to standard error. Statistical differences have been determined with Fisher LSD test following 2-Way ANOVA with p-value < 0.05. Confidence intervals for all pairwise differences between factor levels are indicated by different letters.

doi:10.6342/NTU202301575

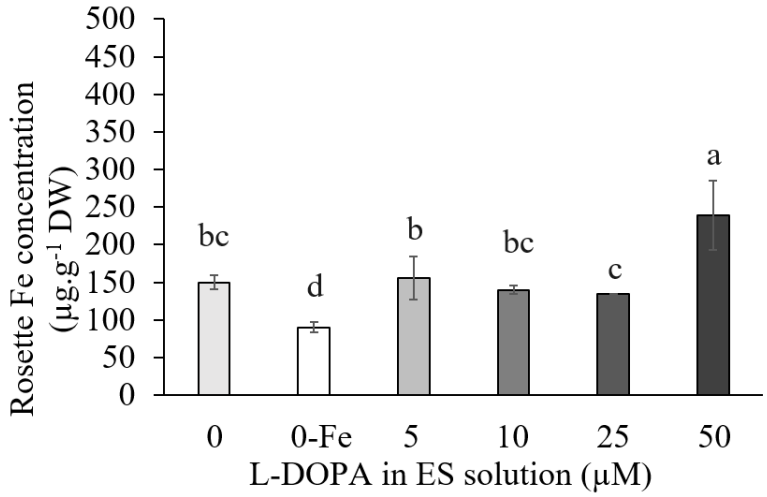

Figure 3.10 | Rosette Fe concentrations of 3-week L-DOPA treated plants.

3-week-old wild type (Col-0) Arabidopsis plants are treated with L-DOPA at concentration 0 (±Fe), 5 (+Fe), 10 (+Fe), 25 (+Fe), and 50 (+Fe) µM for whole of their lifetime. Results are means of 3 replicates, each replicate consists of 3-4 dry plants. Error bars correspond to standard error. Statistical differences have been determined with Fisher LSD test following 2-Way ANOVA with p-value < 0.05. Confidence intervals for all pairwise differences between factor levels are indicated by different letters.

doi:10.6342/NTU202301575

3.5 L-DOPA increases Fe concentration in soil-grown Arabidopsis

3.5.1 L-DOPA decreases rosette biomass but enhances rosette Fe concentration

The weights and Fe concentrations of rosettes from L-DOPA-treated soil-grown plants were measured. L-DOPA has an allelopathic effect, which was also observed in soil-grown plants, although it was not as drastic as in hydroponics. Soil has a buffering capacity and can adsorb allelopathic compounds to some extent. Figure 3.11 and 3.12 shows that the plant size and biomass became smaller as the L-DOPA concentrations increased. At the highest concentration of 3000 μM in irrigation water, Arabidopsis size was the smallest. The plant fresh weight was not significantly different between 1000 μM and 3000 μM L-DOPA treatments. The plants subjected to these two treatments were significantly lighter than control plants and plants exposed to lower L-DOPA concentrations.

The Fe concentration in the rosettes was determined before bolting, which corresponded to 1 month old-plants. Arabidopsis treated with 3000 μM L-DOPA had the highest Fe concentration in their leaves, while there was no significant difference between the other treatments and the control plants (Figure 3.13).

doi:10.6342/NTU202301575

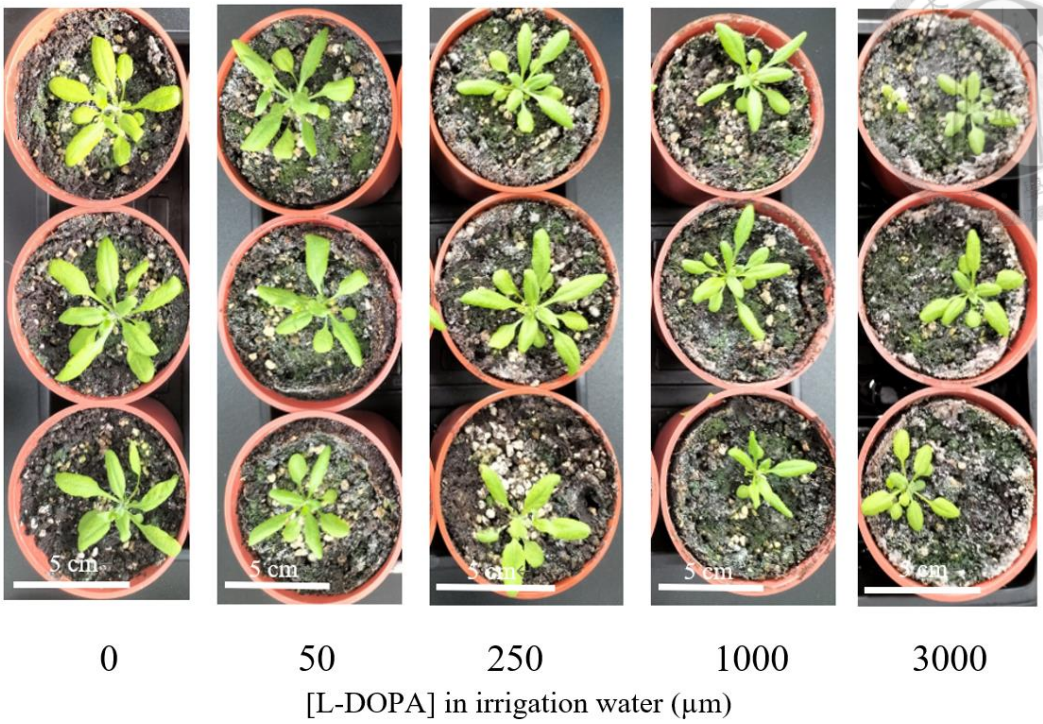

Figure 3.11 | Arabidopsis grown on soil and watered with different concentration of L-DOPA treatments. Arabidopsis plants were grown on potting soil with pH around 5.8. They were watered with 0, 50, 250, 1000, 3000 μM L-DOPA in 100 mL irrigation water once a week from germination. The pictures were taken at 3 to 4 weeks of growth. Scale bar = 5 cm.

doi:10.6342/NTU202301575

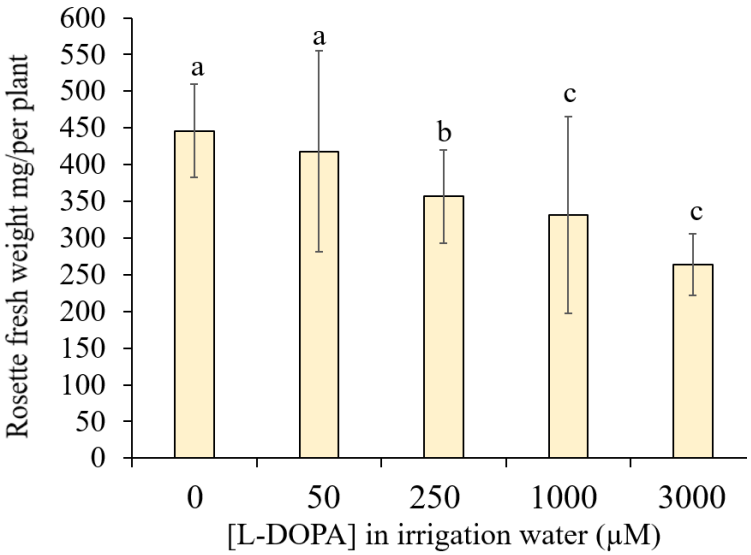

Figure 3.12 | Rosette fresh weights of the Arabidopsis watered with L-DOPA.

Around 4-week-old soil-grown Arabidopsis plants were collected. They were watered with irrigation water containing 0, 50, 250, 1000, 3000 µM L-DOPA once a week throughout their lifetime. Results are means of 5 replicates, each replicate consists of 1 dry plant. Error bars correspond to standard error. Statistical differences have been determined with Fisher LSD test following 2-Way ANOVA with p-value < 0.05. Confidence intervals for all pairwise differences between factor levels are indicated by different letters.

doi:10.6342/NTU202301575

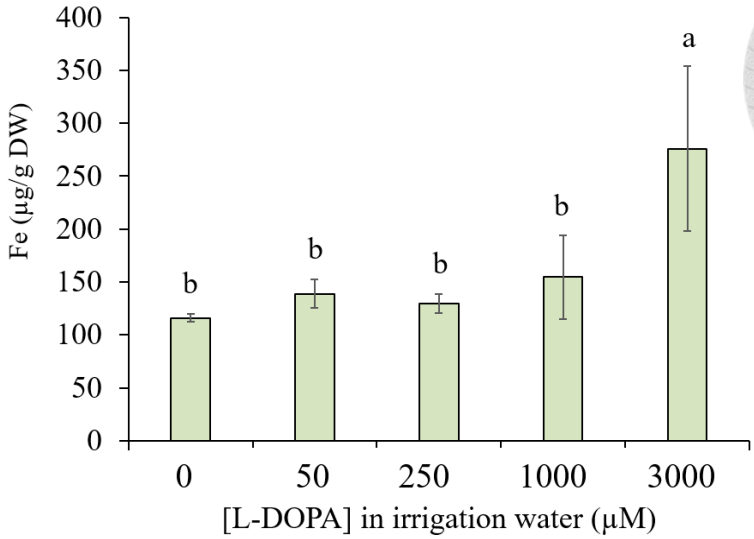

Figure 3.13 | Rosette Fe concentrations of the Arabidopsis watered with L-DOPA.

Around 4-week-old soil-grown Arabidopsis plants were collected. They were watered with irrigation water containing 0, 50, 250, 1000, 3000 µM L-DOPA once a week throughout their lifetime. Results are means of 3 replicates, each replicate consists of 1-2 dry plants. Error bars correspond to standard error. Statistical differences have been determined with Fisher LSD test following 2-Way ANOVA with p-value < 0.05. Confidence intervals for all pairwise differences between factor levels are indicated by different letters.

doi:10.6342/NTU202301575

3.5.2 L-DOPA increases seed Fe content while not severely affecting seed yields

The seeds produced by L-DOPA watered Arabidopsis have more Fe than control (Figure 3.15). When watered with more concentrated L-DOPA, the soil-grown Arabidopsis accumulate more Fe in the seeds. Especially the plants watered with 3000 μM L-DOPA, the seeds of which have up to 3-fold increase in Fe content.

In point 3.4.1 we can see that the rosette sizes and weights of L-DOPA watered Arabidopsis go slightly smaller and lower with the increase in L-DOPA concentrations. However, when the growth time is lengthened to fruiting period, there is no significant visual difference we can tell from no L-DOPA watered plants and L-DOPA watered plants. The plants all look similar at the fruiting stage. This fact reflects on the seed yield (Figure 3.14). The seed yields, except that from 3000 μM L-DOPA watered plants, don't appear a downward trend. Instead, the seed yield of the 1000 μM L-DOPA watered plants is the most abundant. There is also no significant difference in seed yields between 0, 50, 250, 1000 μM L-DOPA watered plants in statistical tests.

doi:10.6342/NTU202301575

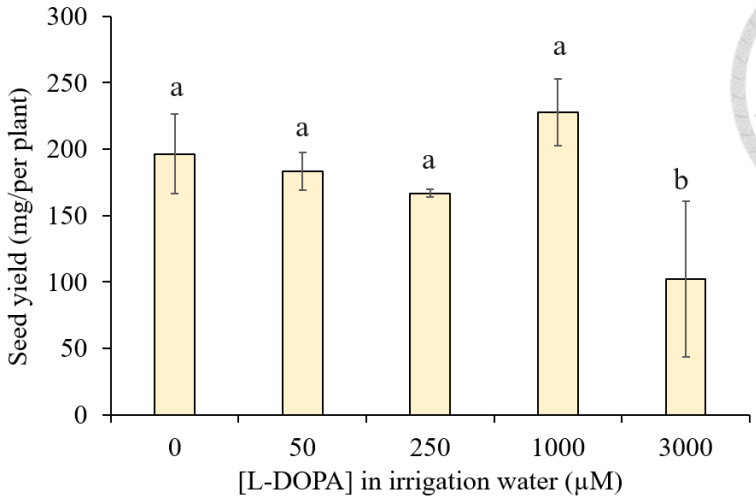

Figure 3.14 | Seed yields of Arabidopsis watered with L-DOPA.

Around 6 or 7-week-old soil-grown Arabidopsis plants were collected. They were watered with irrigation water containing 0, 50, 250, 1000, 3000 μM L-DOPA once a week throughout their lifetime. Results are means of 4 replicates, each replicate consists of seeds form an identical plant. Error bars correspond to standard error. Statistical differences have been determined with Fisher LSD test following 2-Way ANOVA (p-value < 0.05). Confidence intervals for all pairwise differences between factor levels are indicated by different letters.

doi:10.6342/NTU202301575

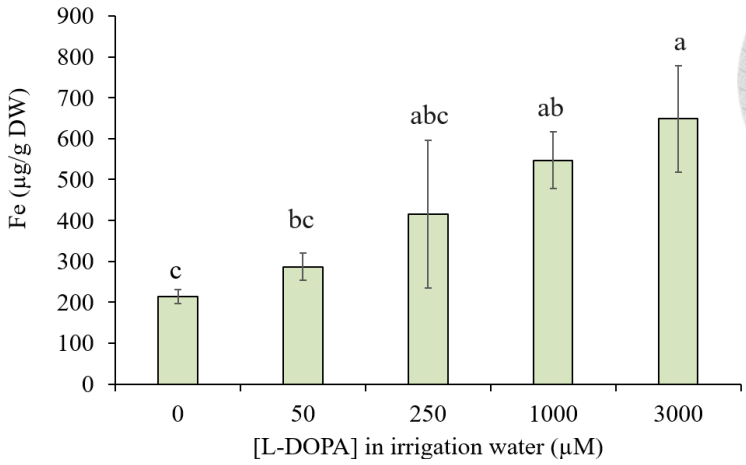

Figure 3.15 | Seed iron concentration of Arabidopsis watered with L-DOPA.

Around 6 or 7-week-old soil-grown Arabidopsis plants were collected. They were watered with irrigation water containing 0, 50, 250, 1000, 3000 µM L-DOPA once a week throughout their lifetime. Results are means of 6 replicates, each replicate consists of around 5 mg of seeds form an identical plant. Error bars correspond to standard error. Statistical differences have been determined with Fisher LSD test following 2-Way ANOVA (p-value < 0.05). Confidence intervals for all pairwise differences between factor levels are indicated by different letters.

doi:10.6342/NTU202301575

3.6 Brief discussion of Part I

To summarize, L-DOPA, though being inhibitory for the growth of Arabidopsis, has the ability to trigger Fe deficiency response. This is demonstrated not only from hydroponic root FCR assay but also from gene expression measured by qPCRs. Because of its ability to trigger Fe uptake, L-DOPA can therefore indeed increase Fe concentration in plant tissues, confirming our main hypothesis. The plants from hydroponic L-DOPA experiments and soil-grown L-DOPA experiments all had higher Fe concentration in their leaves; in soil-grown plants, the L-DOPA-treated plants accumulated more Fe inside the seeds while the seed yield did not decrease drastically.

However, during the series of experiments, we made some interesting observations: 1- there was some variability between experiments which could not be explained by any factor that we controlled. 2- Some of the variability was caused by the solvent used to solubilize L-DOPA prior to treatment. 3- The L-DOPA oxidized at alkaline pH and turned to a brown product believed to be melanin. These observations led us to believe that not only L-DOPA, but also its oxidation products might contribute to plant Fe deficiency response as well.

doi:10.6342/NTU202301575

4. Results—Part II

L-DOPA can be oxidized by several factors *in vivo*. High pH, free metal ions, reactive oxygen species and oxygen all contribute to its oxidation (Figure 4.1). During the experiments, we tried to dissolve L-DOPA in both acidic and basic solutions and we discovered that in acidic environment, L-DOPA solution remains transparent. This was not the case in basic solutions. In basic environment, the color of L-DOPA solution changes over time. With time passing, it sequentially turns orange, brown, dark brown, black. Finally, the L-DOPA solution became sticky and black in basic environment. We suppose that a new molecule was formed from L-DOPA. Indeed, L-DOPA oxidation is known to lead to the formation of DHI and DHICA, and finally melanin. Melanin has a dark color.

doi:10.6342/NTU202301575

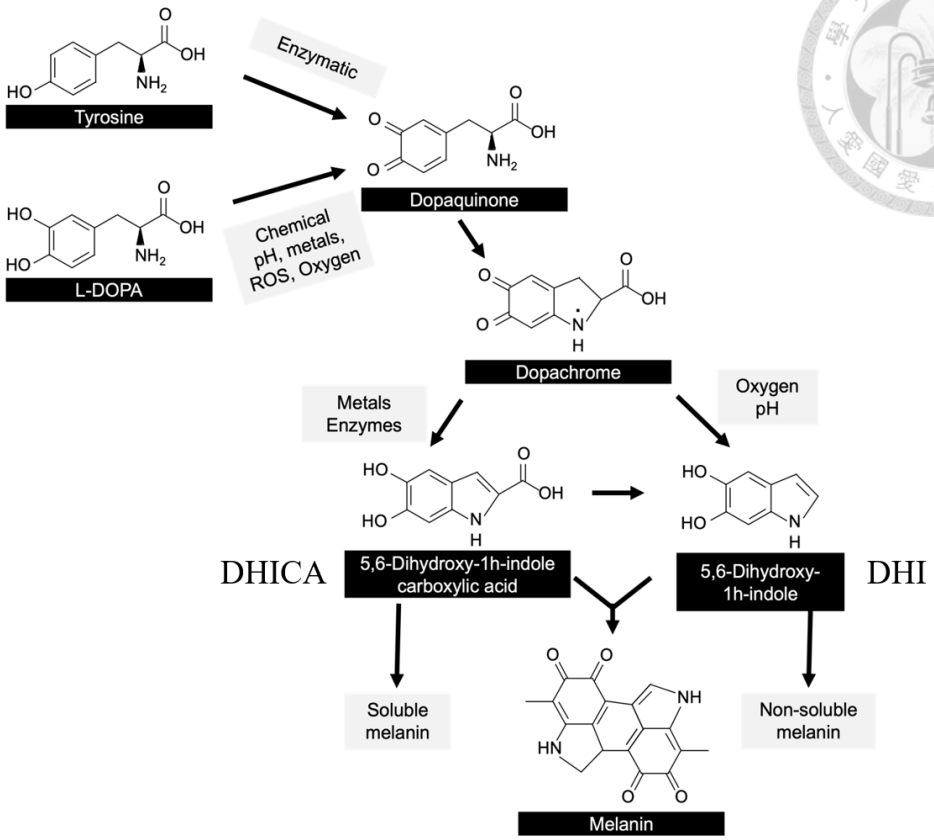

Figure 4.1 | L-DOPA oxidation process. L-DOPA oxidizes through different pathways and finally polymerizes into melanin. The oxidation yields products with dark colors.

doi:10.6342/NTU202301575

pH favorizes L-DOPA oxidation in solution. To investigate the influence of L-DOPA under different pH to plants, we grew Arabidopsis in hydroponic, on ES medium at pH 5.5 and 6, respectively. The plant treated with L-DOPA at pH5.5 had longer ptimary roots than at pH 6 (Figure 4.2). The roots of L-DOPA-treated plants at pH 6 was darker than the roots treated at pH 5.5. This means that this small change in pH also caused an increased in L-DOPA toxicity. Furthermore, it was likely that L-DOPA was more oxidized at pH 6, suggesting that L-DOPA itself might not be inhibiting root growth but that one of its oxidation products might be the cause of the toxicity to Arabidopsis. In order to test this hypothesis, we designed another set of experiments. First, the compounds produced by L-DOPA oxidation in the medium were studied by HPLC. Then, the direct oxidation products of L-DOPA were synthesized, and their bioactivity on Arabidopsis was investigated.

doi:10.6342/NTU202301575

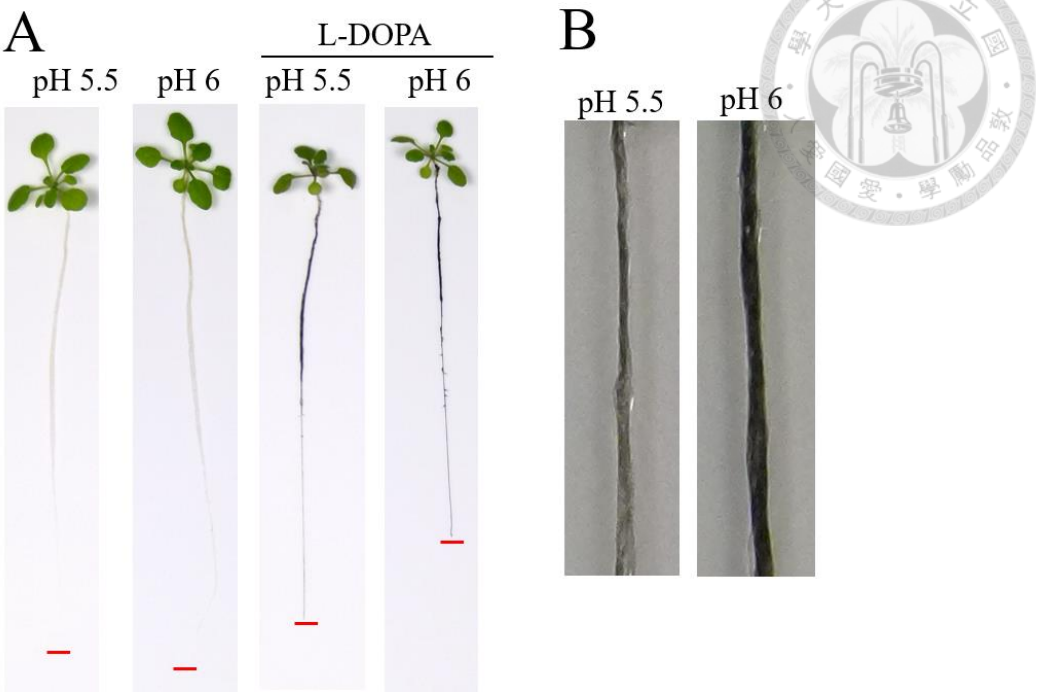

Figure 4.2 | Plants treated with exogenous 250 μM L-DOPA and grown at pH 5.5 and 6 under hydroponics. (A) The pictures of the whole plants; (B) Close-up pictures of the L-DOPA treated roots. Root growths of L-DOPA treated plants under pH 5.5 and 6 are different. The roots of plants grown at pH 6 are shorter and darker. Red lines in (A) represent the position of the primary root tip.

4.1 L-DOPA oxidation in basic condition

As previously discussed, L-DOPA is stable in acidic environments, but is more unstable at high pH. When solubilized in pH 8 KOH solution, L-DOPA becomes oxidized over time. L-DOPA oxidation may yield either DHI and DHICA. All three molecules can be detected by HLPC, and were monitored in a 3 hours L-DOPA

doi:10.6342/NTU202301575

oxidation time-course. Based on the protocol described in Paragraph 2.7.1, L-DOPA could be detected at peak wavelength 282 nm with the retention time around 2.8 minutes; DHI and DHICA could be detected at peak wavelength 300 nm with the retention time around 5.9 minutes and 7.2 minutes, respectively. Throughout the time-course, the area under the peak of L-DOPA gradually decreased, showing that L-DOPA was oxidizing into a different molecule; while DHI appeared temporarily between 10 minutes to 1 hour, the signal then disappears. There is a high probability that part of the oxidized L-DOPA turns into DHI. DHI then oxidizes and polymerizes to DHI oligomers, which are hardly detectable. Throughout 3 hours of observation, no DHICA was detected or is below detection limit of HPLC. This observation shed light on the *in vitro* L-DOPA oxidation process: L-DOPA transiently oxidizes into DHI, which is unstable and in turn, oxidizes too, while DHICA is not produced at a significant level in the conditions tested. DHI oxidation may lead to the formation of other compounds, for example, DOPA-melanin which is not detectable by its absorbance of 300 nm (for DHI & DHICA) and 282 nm (for L-DOPA). DOPA-melanin has been described as a mixture of various DHI oligomers, which spontaneously assembled in different ways.

doi:10.6342/NTU202301575

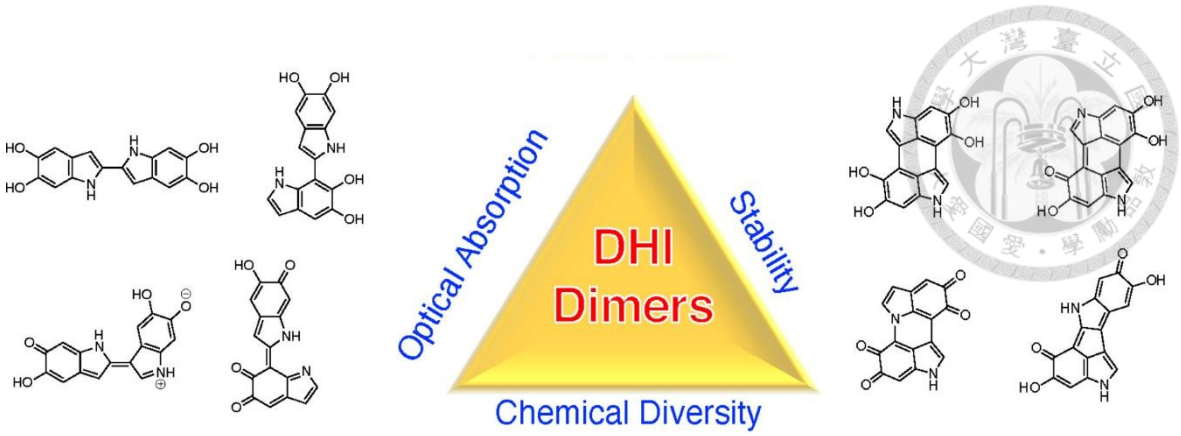

Supplementary Figure S4.3 | Examples of DHI dimers. There are tons of ways for two DHI molecules to dimerize spontaneously. These are just a few examples. (Wang & Blancafort, 2021)

doi:10.6342/NTU202301575

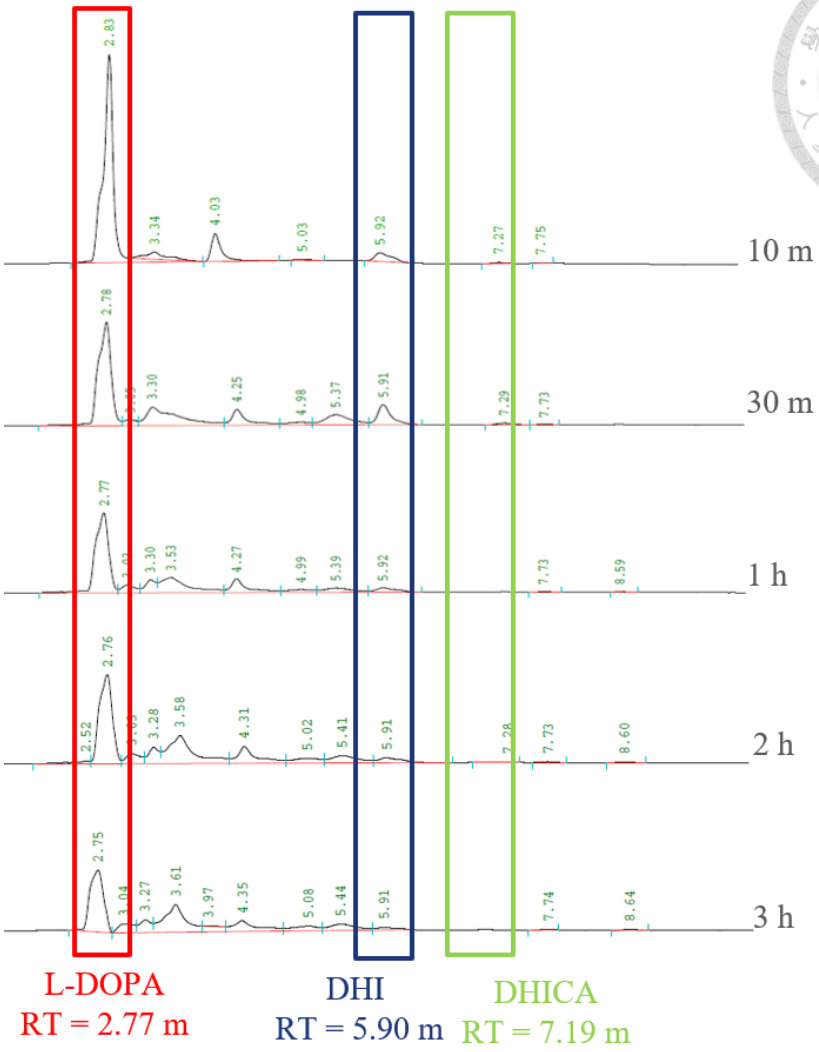

Figure 4.4 | L-DOPA oxidation at pH 8 monitored by HPLC. L-DOPA, DHI and DHICA detection in HPLC. The optimal wavelength for detecting L-DOPA is 282 nm and 300 nm for DHI and DHICA. In this figure, the monitored wavelength for the whole 3 molecules was 282 nm. The retention time of L-DOPA standard was 2.77 min (red box), 5.90 min for DHI standard (blue box), and 7.19 min for DHICA standard (light green box). The time on the right was from the oxidation start upon L-DOPA solubilization. RT, retention time; min, minutes; h, hours.

doi:10.6342/NTU202301575

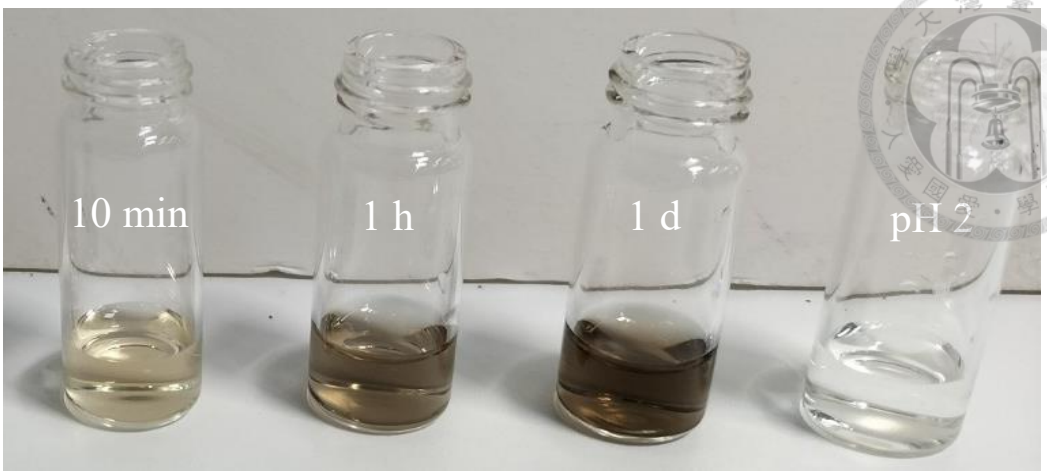

Figure 4.5 | The color changes of L-DOPA serial oxidation. Leftmost, 250 μM L-DOPA in pH 8 KOH for 10 minutes; second from the left, 250 μM L-DOPA in pH 8 KOH for 1 hour; third from the left, 250 μM L-DOPA in pH 8 KOH for 1 day; rightmost, 250 μM L-DOPA dissolved in pH 2 HCl. min = minute; h = hour; d = day.

doi:10.6342/NTU202301575

4.2 Synthesis of high purity DHICA

In the following hydroponic experiments, DHI and DHICA were required in large quantity in order to be exogenously applied to plants in the same way that L-DOPA was. DHI is commercially available and was purchased from a company. Although it is commercially available, DHICA is very expensive and cost approximately 1,000 NT dollars per milligram. We therefore decided to attempt the synthesis of this compound. Synthesis methods are available in the literature. The methods described by Charkoudian and Franz (2006) (See Paragraph 2.6) were implemented in order to produce DHICA. The identity of the homemade compound was confirmed by LC-MS/MS. With LC-MS, we determined that the mass-charge ratio (m/z) of the commercial (standard) DHICA and the synthesized DHICA were identical. MS/MS was used to fragment the ion detected at the m/z corresponding to DHICA, and the fragmentation pattern of the synthesized DHICA was also identical to the certified DHICA standard. Because these two DHICA have an identical fingerprint, we can be certain that they are the same compound. Through LC, using the same mass of material, a stronger signal was detected for the synthesized DHICA as compared to the standard. In other words, the same weight of powder of synthesized DHICA produced a stronger signal than the standard. It was therefore concluded that the purity of the synthesized DHICA was higher than the commercial one, probably due to its oxidation during the

doi:10.6342/NTU202301575

transport and storage.

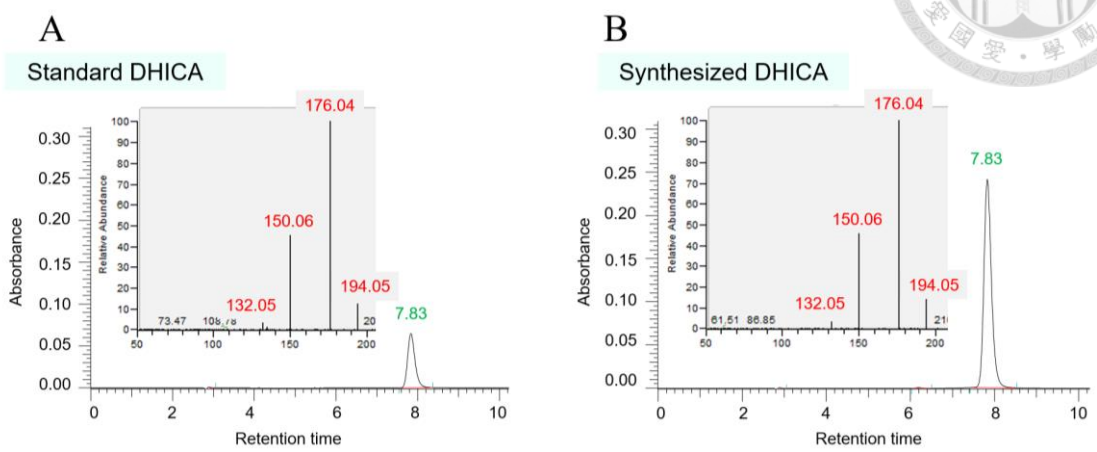

Figure 4.6 | Homemade DHICA has a higher purity than the commercial one. The DHICA standard (A) fragmentizes in ions with 132.05, 150.06, 176.04 and 194.05 mass-charge ratios (m/z). The synthesized DHICA (B) has an identical fingerprint. The retention time of both DHICA are 7.83 minutes, while for the same theoretical concentration of 10 ppm, the synthesized DHICA produced a larger peak.

doi:10.6342/NTU202301575

4.3 L-DOPA and its indolic derivatives have similar effects on root FCR activity

In this experiment, the effect of 3 compounds and L-DOPA on Arabidopsis were tested. The compounds consisted of L-DOPA indolic derivatives DHI, DHICA and a non-catecholic structural analogue of DHICA, 5-hydroxyindole-2-carboxylic acid (HICA). The only difference between DHICA and HICA is that HICA harbors only one hydroxyl group on the 5th carbon of its indole ring, and no hydroxyl group on the 6th carbon.

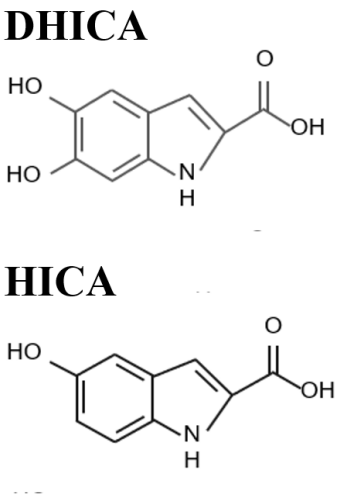

Supplementary Figure S4.7 | DHICA and HICA. HICA is a DHICA analogue. The only difference between the two compounds is that HICA harbors only one hydroxyl group on the 5th carbon of the indole ring while DHICA have two hydroxyl groups on the 5th and 6th carbons.

doi:10.6342/NTU202301575

The physiological behavior of the Arabidopsis treated with the different compounds are shown in Figure 4.6. The roots of the melanin precursor-treated plants turned black, as expected because these precursors ultimately oxidize into melanin and sticks on the root surface. HICA is not one of the melanin precursors, and therefore the roots treated with it did not become black, although they were not as white as the roots of untreated plants. In fact, HICA-treated roots were slightly brownish, which may indicate the formation of an unknown brown compound, possibly lignin. All the indole-treated roots grew shorter than control, showing the inhibitory nature of these compounds. The adaxial and abaxial sides of the leaves were captured by camera. All the compound-treated rosettes were visibly smaller than control. Interestingly, leaves of L-DOPA and DHI treated plants had a darker, purple color. The cause of this phenomenon was hypothesized to be anthocyanin accumulation in the leaves, thus the anthocyanin was quantified (Figure 4.9). The content of anthocyanin in the leaves of L-DOPA and DHI treated plants are is higher than in plants subjected to other treatments. For plants, anthocyanin is generally considered as a marker of stress, and we therefore concluded that L-DOPA and DHI cause a stress to the leaves, thereby leading to anthocyanin formation.

FCR assays of roots of plants treated with the investigated compounds were measured (Figure 4.10). A trend was revealed by FCR assays — compared to control,

doi:10.6342/NTU202301575

all the compound-treated plants had higher FCR activities under Fe sufficient conditions, except for HICA, with which the root FCR activity was not statistically different as compared to control; on the other hand, when Fe is deficient in the environment, the addition of all the compounds to the media decreased root FCR activities. This means that the intermediates of L-DOPA oxidation can boost Fe uptake capacity when Fe is sufficient, however, in Fe deficient conditions, they repress root Fe deficiency response.

doi:10.6342/NTU202301575

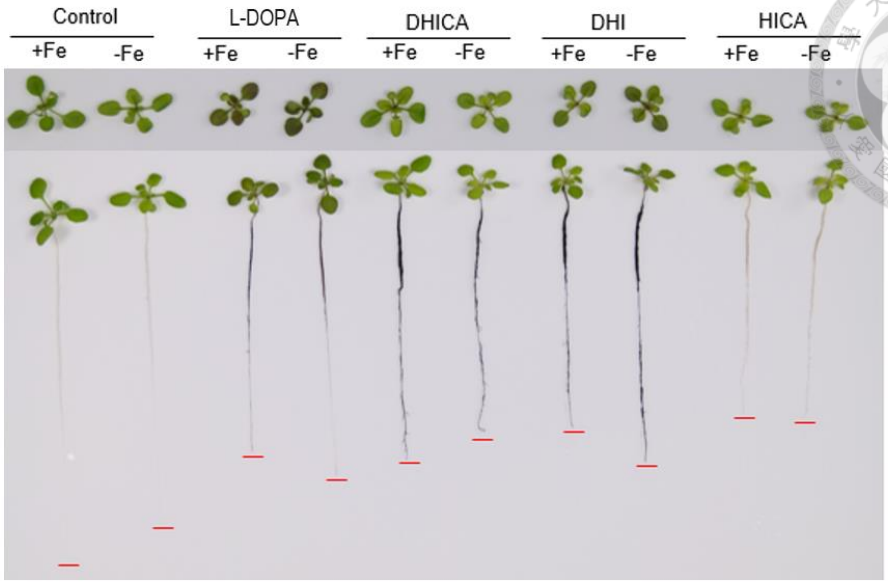

Figure 4.8 | Phenotypes of Arabidopsis treated with L-DOPA, DHICA, DHI and HICA in hydroponics. The photos were taken after 2 weeks of plant growth in normal ES solution (pH 5.5) and 3 days of different compound treatments all at the concentration of 250 μM. During the 3-day treatments, a half of plants were treated under normal Fe supplement (+ Fe) while another half were treated with Fe-EDTA removed from the medium and added with FerroZine (– Fe). Red lines represent the position of the primary root tip. Upper row shows the abaxial side of the plants. Scale bar = 1 cm.

doi:10.6342/NTU202301575

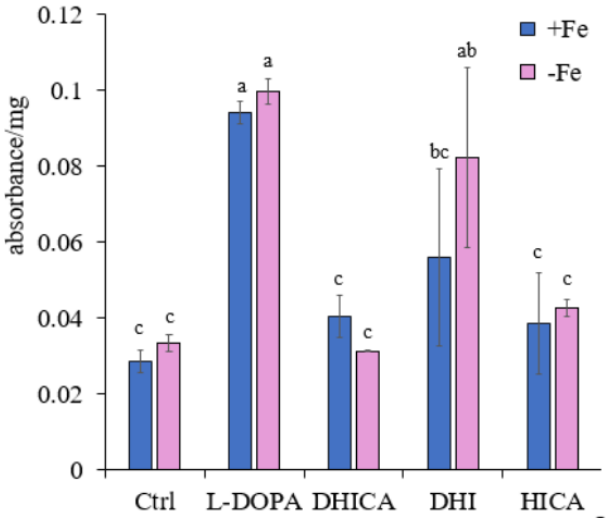

Figure 4.9 | Anthocyanin concentration in rosettes of hydroponic Arabidopsis treated with L-DOPA, DHICA, DHI and HICA. Hydroponically grown 2-week-old Arabidopsis plants were treated with 250 µM L-DOPA, DHICA, DHI and HICA. The treatments were implemented with a half of plant subjected to normal nutrient solution recipe (+Fe) and another half subjected to Fe deficient recipe with FerroZine (– Fe). Results are means of 2 replicates each treatment, each replicate consists of 1-2 freeze-dried rosettes. Error bars correspond to standard error. Statistical differences were determined using Fisher's LSD test following 2-way ANOVA with p-value < 0.05. Confidence intervals for all pairwise differences between factor levels are indicated by different letters.

doi:10.6342/NTU202301575

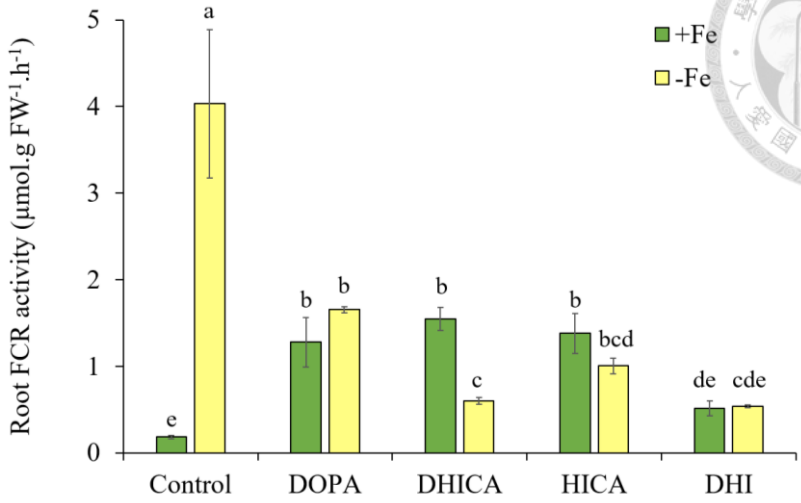

Figure 4.10 | Root FCR activities of hydroponic Arabidopsis treated with L-DOPA, DHICA, DHI and HICA. Hydroponically grown 2-week-old Arabidopsis plants were treated with 250 μM L-DOPA, DHICA, DHI and HICA. The treatments were implemented with a half of plants subjected to normal nutrient solution recipe (+Fe) and another half subjected to Fe deficient recipe with FerroZine (– Fe). Results are means of 2 independent boxes of plants, 3-4 plants among the 12 plants per box is a replicate. Error bars correspond to standard error. Statistical differences were determined using Fisher's LSD test following 2-way ANOVA (p-value < 0.05). Confidence intervals for all pairwise differences between factor levels are indicated by different letters.

doi:10.6342/NTU202301575

4.4 Fully oxidized L-DOPA acts differently than L-DOPA

3 days after solubilization of L-DOPA at high pH, no L-DOPA, DHI, nor DHICA could be observed by HPLC. We therefore decided to test the effect of this solution, called "oxidized L-DOPA" on Arabidopsis. In order to study the ultimate oxidation products of L-DOPA on Arabidopsis, L-DOPA was dissolved at pH 8 for 72 hours, and we checked that L-DOPA, DHI and DHICA were not detectable anymore. This solution was applied to plants for 3 days. Subsequently, the rosette fresh weight and root FCR activity were measured.

Surprisingly, the “fully oxidized” L-DOPA loses the L-DOPA inhibitory properties. First, as shown in Figure 4.11, independently of the presence of Fe in the nutrient solution, the addition of fully oxidized L-DOPA did not inhibit the growth of Arabidopsis. In Fe-replete medium, there was no significant difference between the rosette biomass of control plants and those treated with the fully oxidized L-DOPA; in Fe-deplete condition, rosette fresh weights of the fully oxidized L-DOPA-treated plants were even higher than those of controls. These results show that fully oxidized L-DOPA did not inhibit plant growth.

Second, through FCR assay (Figure 4.12) we observed that in presence of Fe, fully oxidized L-DOPA did not trigger the increase of FCR activity; furthermore, under Fe deficiency, the plants treated with fully oxidized L-DOPA did not increase their FCR

doi:10.6342/NTU202301575

activity, which should have been the expected Fe deficiency response. According to the conclusion from paragraph 4.3, non-oxidized L-DOPA triggers Fe uptake when Fe is sufficient and repress Fe deficiency response when Fe is insufficient in the environment. This was not the case for the oxidized L-DOPA, although liked L-DOPA, the oxidized L-DOPA retained the ability to inhibit Fe deficiency response in Fe-deficient plants. However, the specific molecules remaining in the flask after 72 hours of L-DOPA oxidation are not identified. We can exclude the possibility that it is L-DOPA, DHI or DHICA. There is a high possibility that the compound remained in the flask is a mixture of DHI oligomers, called DOPA-melanin. There are many of these oligomers, with different structures, and the study of these compounds is notoriously difficult.

doi:10.6342/NTU202301575

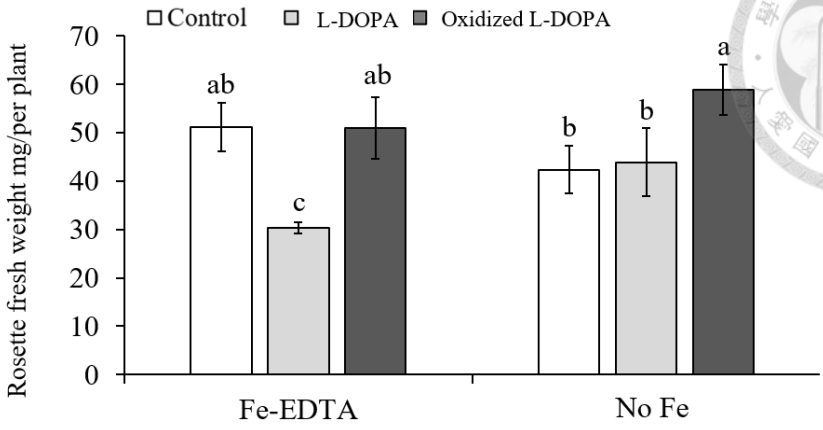

Figure 4.11 | Rosette biomass of Arabidopsis grown in hydroponics and subjected to L-DOPA and oxidized DOPA treatments. Arabidopsis plants were grown for two weeks and treated with normal ES medium/ ES medium plus 250 µM fresh L-DOPA/ ES medium plus 250 µM fully oxidized L-DOPA for another 3 days. The treatments were implemented with a half of plants subjected to normal nutrient solution recipe (Fe-EDTA) and another half subjected to Fe deficient recipe with FerroZine (No Fe). Results are means of 3 biological replicates each, a replicate is an Arabidopsis rosette. Error bars correspond to standard error. The multiple comparison method used is Fisher's LSD with p-value < 0.05. Confidence intervals for all pairwise differences between factor levels are indicated by different letters.

doi:10.6342/NTU202301575

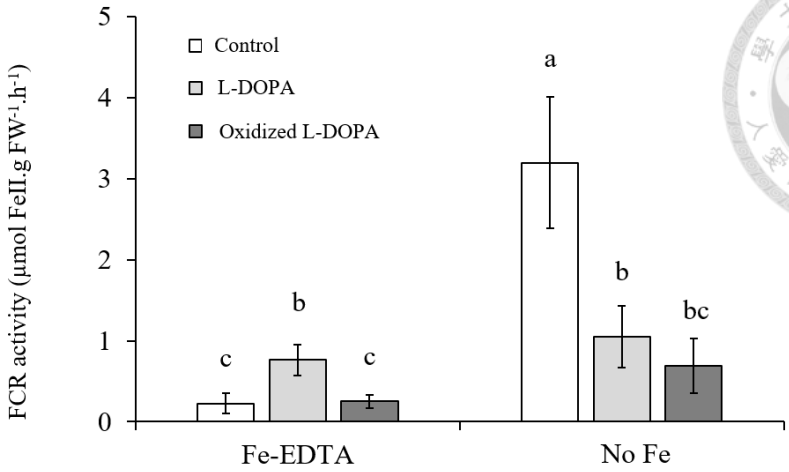

Figure 4.12 | Root FCR activities of Arabidopsis grown in hydroponics and subjected to L-DOPA and oxidized DOPA treatments. Arabidopsis plants were grown for two weeks and treated with normal ES medium/ ES medium plus 250 μM fresh L-DOPA/ ES medium plus 250 μM fully oxidized L-DOPA for another 3 days. The treatments were implemented with a half of plants subjected to normal nutrient solution recipe (Fe-EDTA) and another half subjected to Fe deficient recipe with FerroZine (No Fe). Results are means of 3 independent boxes, , 3-4 plants among the 12 plants per box is a replicate. Error bars correspond to standard error. The multiple comparison method used is Fisher's LSD with p-value < 0.05. Confidence intervals for all pairwise differences between factor levels are indicated by different letters.

doi:10.6342/NTU202301575

5. Discussion

5.1 L-DOPA application enables plants to take up more Fe

We know from the research by Golisz et al in 2011 that hydroponic L-DOPA treatment highly induces the expression level of *AtIMA1* (Golisz et al., 2011). In our research, we not only performed FCR assays but also qPCRs to measure the expression of the Fe uptake genes *AtIRT1* and *AtFRO2*. From the results of these experiments, we can tell that even though the environment has sufficient Fe, L-DOPA can still induce the expression of *AtIRT1* and *AtFRO2*. L-DOPA induces a large increase in IMA1expression, and subsequently, IRT1 and FRO2 are activated by the IMA1 cascade under Fe sufficient condition. This leads to more Fe accumulation in Arabidopsis tissues like seeds and rosettes. The optimal L-DOPA concentration to increase Arabidopsis Fe uptake is at 50 or 100 μM in hydroponic system; in soil the effect of L-DOPA was mitigated, and concentrations of 1000 to 3000 μM of L-DOPA was optimal. L-DOPA triggered Fe uptake and inhibited the growth of plants. After all, it is an allelopathic compound and cannot be applied in too large amount, but L-DOPA undoubtedly has the ability to increase Fe uptake.

doi:10.6342/NTU202301575

5.2 L-DOPA is not redundant with EDTA

EDTA is a widely used Fe chelator which increases Fe solubility and therefore its bioavailability. EDTA can be used to increase Fe concentration in crops although it is a synthetic molecule which is costly and might cause environmental damages when used on a large scale. In fact, EDTA is considered one of the major organic pollutants discharged in water (Sillanpaa, 1997). In previous experiments (paragraph 3.3.1.), we showed that L-DOPA and EDTA have distinct effects and can act synergistically in the way they affect plant Fe uptake. EDTA keeps Fe soluble and prevent it from oxidizing L-DOPA; on the other hand, L-DOPA forces the plant to maintain a high Fe uptake regardless of its Fe status. These two compounds have non redundant effects on the plant, and these effects can even be additive. If both molecules are applied to plants, the increase in Fe concentration will likely be much higher as compared to when there is only EDTA or only L-DOPA.

doi:10.6342/NTU202301575

5.3 L-DOPA or its oxidation products, which trigger the Fe deficiency response?

As mentioned in the introduction, L-DOPA has two major oxidation products DHI and DHICA (Figure 4.1). These two L-DOPA products are very unstable and prone to oxidize and oligomerize to produce melanin. We would like to know whether L-DOPA itself or its products trigger Arabidopsis Fe uptake, because L-DOPA readily oxidizes in basic or metal-containing environments. In our experiments, L-DOPA oxidizes into melanin precursors, prominently DHI, and ultimately DOPA-melanin in the nutrient solution. DHICA was not detected on HPLC during our oxidation time-course. After the plants were treated with L-DOPA, DHI, DHICA, and HICA, we discovered that all the melanin precursors and HICA can decrease the response of Fe deficient plants. In contrast, only L-DOPA, DHI and DHICA, all of which harbor a catechol group, did increase the FCR activity of Fe-sufficient plants. Both L-DOPA and DHI induced anthocyanin production in the leaves, whereas DHICA and HICA did not have a significant effect: indeed, Arabidopsis plants treated with high concentrations of L-DOPA had darker leaves (Figure 3.2), and DHI-treated plants as well (Figure 4.8). To conclude, these evidences may imply that the effects of L-DOPA and DHI might be related, and that L-DOPA oxidation yields DHI, rather than DHICA in our conditions. The mixture of fully oxidized DOPA resulted in an inhibition of Fe deficiency response

doi:10.6342/NTU202301575

of plants subjected to a Fe-deplete medium, similar to what was observed with all the other molecules. It is therefore plausible that all the melanin precursors oxidized to similar oligomers and that these oligomers have a negative effect on Fe uptake and Fe deficiency response.

5.4 L-DOPA should be replenished to maintain high Fe uptake of plants

When L-DOPA was oxidized for 72 hours and yielded a sticky, dark solution, which was called “oxidized L-DOPA” and likely corresponds to melanochrome, i.e. a mixture of oligomers of the indolic precursors of eumelanin. After exogenously applying the oxidized L-DOPA to Arabidopsis, we discovered the plants grow even bigger than non-treated ones. L-DOPA is known to be allelopathic, however after being fully oxidized, it is no longer able to inhibit the growth of Arabidopsis. Fully oxidized L-DOPA did not stimulate Fe uptake but it did inhibit the induction of root FCR activity in Fe-deficient plants. Further investigation is needed to identify the exact compound(s) produced from L-DOPA oxidation which is mediating this inhibition. However, we can be sure that this material did not contain any L-DOPA and did not have the same properties as L-DOPA. In order to apply L-DOPA to crops and increase their Fe uptake, L-DOPA would need to be replenished regularly. In hydroponics the replenishment

doi:10.6342/NTU202301575

consists in replacing the nutrient solution with a newly prepared L-DOPA-containing medium, while for the soil grown plants, a strategy of intercropping with a L-DOPA-producing plant, or inoculation with melanin-producing plant growth promoting rhizobacteria (PGPR) would be the most appropriate approach.

5.5 Novel repressors for Fe deficiency response are revealed

As aforementioned in Paragraph 1.4, there are 2 small molecules R3 (N-[4-(1,3-benzothiazol-2-yl)-2-methylphenyl] acetamide) and R6 (2-benzoyl-1-benzofuran-5-carboxylic acid) reportedly to suppress Fe deficiency response in *Arabidopsis thaliana*. This present thesis reveals another 2 molecules which also block Fe uptake capacity conditionally in Fe-deplete condition. DHI and DHICA trigger Fe uptake in Fe-replete environment while inhibiting Fe uptake during Fe deficiency. There might be more inhibitors for Fe deficiency response in the downstream of DHI and DHICA oxidation and oligomerization, i.e., melanochrome. However, to elucidate which types of oligomers give rise to Fe uptake inhibition is another task to investigate.

doi:10.6342/NTU202301575

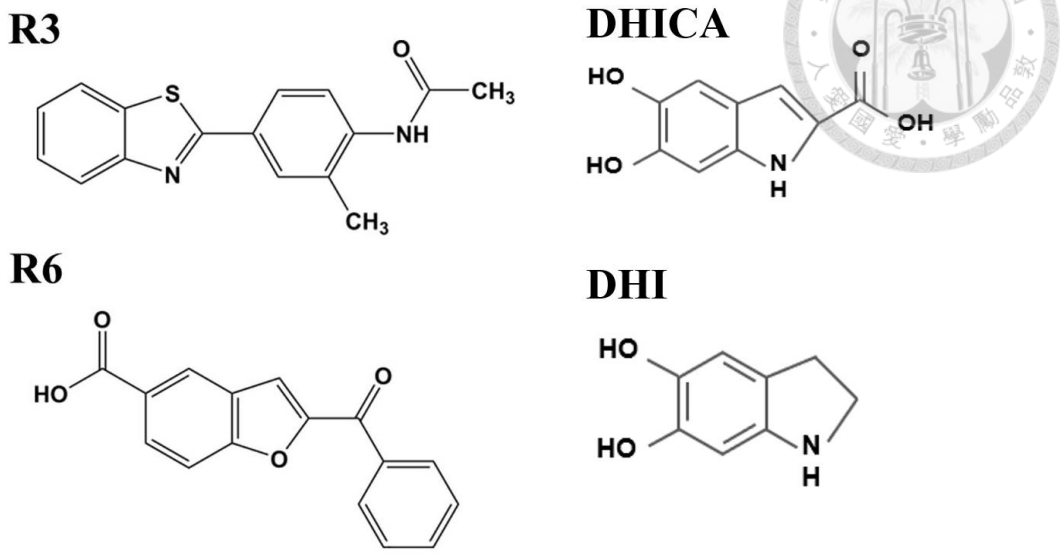

Supplementary Figure S5.1 | Comparison between R3, R6, DHICA and DHI. There are some structurally similarities between these 4 molecules shown. Broadly speaking, they are all Fe uptake inhibitors (Kailasam et al., 2019).

doi:10.6342/NTU202301575

6. Conclusion

As iron deficiency anemia (IDA) becomes increasingly widespread worldwide, strategies to tackle low Fe content in crops need to be developed. In this present study, we tested the feasibility of using L-DOPA as a biostimulant for plant Fe biofortification. Through researches, we established the fact that L-DOPA being a biostimulant for plant Fe biofortification is indeed plausible. In soil-free hydroponics, the addition of L-DOPA enhances FCR activity of Arabidopsis roots, and also boost leaf Fe concentration to more than two folds when applied adequately; in soil, 3000 μM of L-DOPA in irrigation water applied to Arabidopsis enabled the plants to accumulate Fe in the seeds up to three folds the level of control. Despite the fact that L-DOPA becomes oxidized under certain conditions and its application needs replenishment, we can still adopt strategies such as intercropping a target crop with L-DOPA secreting plants to solve the problem. The present research is a pioneering study of this topic, and reveals that this approach is encouraging and promising.

doi:10.6342/NTU202301575

7. References

Bashir, K., Inoue, H., Nagasaka, S., Takahashi, M., Nakanishi, H., Mori, S., & Nishizawa, N. K. (2006). Cloning and characterization of deoxymugineic acid synthase genes from graminaceous plants. *Journal of Biological Chemistry 281*(43): 32395-32402.

Beard, J. (2003). Iron deficiency alters brain development and functioning. *The Journal of Nutrition 133*(5): 1468S-1472S.

Beard, J. L. (2001). Iron biology in immune function, muscle metabolism and neuronal functioning. *The Journal of Nutrition 131*(2): 568S-580S.

Billings, J. L., Gordon, S. L., Rawling, T., Doble, P. A., Bush, A. I., Adlard, P. A., Finkelstein, D. I., & Hare, D. J. (2019). l-3, 4-dihydroxyphenylalanine (l-DOPA) modulates brain iron, dopaminergic neurodegeneration and motor dysfunction in iron overload and mutant alpha-synuclein mouse models of Parkinson's disease. *Journal of Neurochemistry 150*(1): 88-106.

Birkmayer, W., & Hornykiewicz, O. (1961). The L-3, 4-dioxyphenylalanine (DOPA)-effect in Parkinson-akinesia. *Wiener klinische Wochenschrift 73*: 787-788.

Brabin, B. J., Hakimi, M., & Pelletier, D. (2001). An analysis of anemia and pregnancy-related maternal mortality. *The Journal of Nutrition 131*(2S-2): 604S-

doi:10.6342/NTU202301575

614S; discussion 614S.

Cakmak, I., Ozkan, H., Braun, H., Welch, R., & Romheld, V. (2000). Zinc and iron concentrations in seeds of wild, primitive, and modern wheats. *Food and Nutrition Bulletin 21*(4): 401-403.

Calvo, P., Nelson, L., & Kloepper, J. W. (2014). Agricultural uses of plant biostimulants. *Plant and Soil 383*(1): 3-41.

Charkoudian, L. K., & Franz, K. J. (2006). Fe (III)-coordination properties of neuromelanin components: 5, 6-dihydroxyindole and 5, 6-dihydroxyindole-2-carboxylic acid. *Inorganic Chemistry 45*(9): 3657-3664.

Clark, R. B. (1982). Iron deficiency in plants grown in the Great Plains of the US. *Journal of Plant Nutrition 5*(4-7): 251-268.

De Valença, A., Bake, A., Brouwer, I., & Giller, K. (2017). Agronomic biofortification of crops to fight hidden hunger in sub-Saharan Africa. *Global Food Security 12*: 8-14.

Denic, S., & Agarwal, M. M. (2007). Nutritional iron deficiency: an evolutionary perspective. *Nutrition 23*(7-8): 603-614.

Dona, A., & Arvanitoyannis, I. S. (2009). Health risks of genetically modified foods. *Critical Reviews in Food Science and Nutrition 49*(2): 164-175.

Du Jardin, P. (2015). Plant biostimulants: Definition, concept, main categories and

doi:10.6342/NTU202301575

regulation. *Scientia Horticulturae 196*: 3-14.

Eide, D., Broderius, M., Fett, J., & Guerinot, M. L. (1996). A novel iron-regulated metal transporter from plants identified by functional expression in yeast. *Proceedings of the National Academy of Sciences 93*(11): 5624-5628.

Ems, T., St Lucia, K., & Huecker, M. R. (2021). Biochemistry, iron absorption. In *StatPearls [Internet]*. StatPearls Publishing.

Estelle, M. A., & Somerville, C. (1987). Auxin-resistant mutants of Arabidopsis thaliana with an altered morphology. *Molecular and General Genetics MGG 206*: 200-206.

Fourcroy, P., Tissot, N., Gaymard, F., Briat, J.-F., & Dubos, C. (2016). Facilitated Fe nutrition by phenolic compounds excreted by the Arabidopsis ABCG37/PDR9 transporter requires the IRT1/FRO2 high-affinity root Fe^{2+} transport system. *Molecular Plant 9*(3): 485-488.

Franceschi, F., & Gasbarrini, A. (2007). Helicobacter pylori and extragastric diseases. *Best Practice & Research Clinical Gastroenterology 21*(2): 325-334.

Frey, P. A., & Reed, G. H. (2012). The ubiquity of iron. *ACS Chemical Biology 7*(9): 1477-1481.

Gao, F., Robe, K., Bettembourg, M., Navarro, N., Rofidal, V., Santoni, V., Gaymard, F., Vignols, F., Roschzttardtz, H., & Izquierdo, E. (2020). The

doi:10.6342/NTU202301575

transcription factor bHLH121 interacts with bHLH105 (ILR3) and its closest homologs to regulate iron homeostasis in Arabidopsis. *The Plant Cell 32*(2): 508-524.

García-Bañuelos, M. L., Sida-Arreola, J. P., & Sánchez, E. (2014). Biofortification-promising approach to increasing the content of iron and zinc in staple food crops. *Journal of Elementology 19*(3).

Gessler, N., Egorova, A., & Belozerskaya, T. (2014). Melanin pigments of fungi under extreme environmental conditions. *Applied Biochemistry and Microbiology 50*: 105-113.

Golisz, A., Sugano, M., Hiradate, S., & Fujii, Y. (2011a). Microarray analysis of Arabidopsis plants in response to allelochemical L-DOPA. *Planta 233*(2): 231-240.

Golisz, A., Sugano, M., Hiradate, S., & Fujii, Y. (2011b). Microarray analysis of Arabidopsis plants in response to allelochemical L-DOPA. *Planta 233*: 231-240.

Goto, F., Yoshihara, T., Shigemoto, N., Toki, S., & Takaiwa, F. (1999). Iron fortification of rice seed by the soybean ferritin gene. *Nature Biotechnology 17*(3): 282-286.

Graham, R., Senadhira, D., Beebe, S., Iglesias, C., & Monasterio, I. (1999). Breeding for micronutrient density in edible portions of staple food crops:

doi:10.6342/NTU202301575

conventional approaches. *Field Crops Research 60*(1-2): 57-80.

Grillet, L., Lan, P., Li, W., Mokkapati, G., & Schmidt, W. (2018). IRON MAN is a ubiquitous family of peptides that control iron transport in plants. *Nature Plants 4*(11): 953-963.

Grillet, L., Mari, S., & Schmidt, W. (2014). Iron in seeds–loading pathways and subcellular localization. *Frontiers in Plant Science 4*: 535.

Gupta, C. (2014). Role of iron (Fe) in body. *IOSR Journal of Applied Chemistry 7*(11): 38-46.

Haas, J. D., & Brownlie IV, T. (2001). Iron deficiency and reduced work capacity: a critical review of the research to determine a causal relationship. *The Journal of Nutrition 131*(2): 676S-690S.

Heath, C. W., Strauss, M. B., & Castle, W. B. (1932). Quantitative aspects of iron deficiency in hypochromic anemia:(The parenteral administration of iron). *The Journal of Clinical Investigation 11*(6): 1293-1312.

Hindt, M. N., & Guerinot, M. L. (2012). Getting a sense for signals: regulation of the plant iron deficiency response. *Biochimica et Biophysica Acta (BBA)-Molecular Cell Research 1823*(9): 1521-1530.

Hurrell, R., & Egli, I. (2010). Iron bioavailability and dietary reference values. *The American Journal of Clinical Nutrition 91*(5): 1461S-1467S.

doi:10.6342/NTU202301575

Itou, T., Ito, S., & Wakamatsu, K. (2019). Effects of aging on hair color, melanosome morphology, and melanin composition in Japanese females. *International Journal of Molecular Sciences 20*(15): 3739.

Kailasam, S., Chien, W.-F., & Yeh, K.-C. (2019). Small-molecules selectively modulate iron-deficiency signaling networks in Arabidopsis. *Frontiers in Plant Science 10*: 8.

Kappler, A., & Straub, K. L. (2005). Geomicrobiological cycling of iron. *Reviews in Mineralogy and Geochemistry 59*(1): 85-108.

Kauffman, G. L., Kneivel, D. P., & Watschke, T. L. (2007). Effects of a biostimulant on the heat tolerance associated with photosynthetic capacity, membrane thermostability, and polyphenol production of perennial ryegrass. *Crop Science 47*(1): 261-267.

Kobayashi, T., & Nishizawa, N. K. (2012). Iron uptake, translocation, and regulation in higher plants. *Annual Review of Plant Biology 63*: 131-152.

Kok, A. D.-X., Yoon, L. L., Sekeli, R., Yeong, W. C., Yusof, Z. N. B., Song, L. K., Shah, F., Kahn, Z., & Iqbal, A. (2018). Iron biofortification of rice: progress and prospects. *F. Shah, ZH Khan and A. Iqbal (Norderstedt: IntechOpen*: 25-44.

Kong, K. H., Lee, J. L., Park, H. J., & Cho, S. H. (1998). Purification and characterization of the tyrosinase isozymes of pine needles. *IUBMB Life 45*(4):

doi:10.6342/NTU202301575

717-724.

Kulma, A., & Szopa, J. (2007). Catecholamines are active compounds in plants. *Plant Science 172*(3): 433-440.

López-Arredondo, D. L., Leyva-González, M. A., Alatorre-Cobos, F., & Herrera-Estrella, L. (2013). Biotechnology of nutrient uptake and assimilation in plants. *International Journal of Developmental Biology 57*(6-7-8): 595-610.

Li, Y., Lu, C. K., Li, C. Y., Lei, R. H., Pu, M. N., Zhao, J. H., Peng, F., Ping, H. Q., Wang, D., & Liang, G. (2021). IRON MAN interacts with BRUTUS to maintain iron homeostasis in Arabidopsis. *Proceedings of the National Academy of Sciences 118*(39): e2109063118.

Lichtblau, D. M., Schwarz, B., Baby, D., Endres, C., Sieberg, C., & Bauer, P. (2022). The iron deficiency-regulated small protein effector FEP3/IRON MAN1 modulates interaction of BRUTUS-LIKE1 with bHLH subgroup IVc and POPEYE transcription factors. *Frontiers in Plant Science 13*.

Livak, K. J., & Schmittgen, T. D. (2001). Analysis of relative gene expression data using real-time quantitative PCR and the $2^{-\Delta\Delta CT}$ method. *Methods 25*(4): 402-408.

Loeppert, R., & Hallmark, C. (1985). Indigenous soil properties influencing the availability of iron in calcareous soils. *Soil Science Society of America Journal*

doi:10.6342/NTU202301575

49(3): 597-603.

Lozoff, B., Corapci, F., Burden, M. J., Kaciroti, N., Angulo-Barroso, R., Sazawal, S., & Black, M. (2007). Preschool-aged children with iron deficiency anemia show altered affect and behavior. *The Journal of Nutrition 137*(3): 683-689.

Ma, J. F., Taketa, S., Chang, Y.-C., Iwashita, T., Matsumoto, H., Takeda, K., & Nomoto, K. (1999). Genes controlling hydroxylations of phytosiderophores are located on different chromosomes in barley (*Hordeum vulgare L.*). *Planta 207*: 590-596.

Mallik, I., Azim, U. (2002). Chemical ecology of plants: allelopathy in aquatic and terrestrial ecosystems. Birkhäuser Basel. *Springer*.

Marschner, H. (1995). Mineral nutrition of higher plants 2nd edn. Academic Press, London. Institute of Plant Nutrition University of Hohenheim, Germany.

Monsen, E. R., Hallberg, L., Layrisse, M., Hegsted, D. M., Cook, J., Mertz, W., & Finch, C. A. (1978). Estimation of available dietary iron. *The American Journal of Clinical Nutrition 31*(1): 134-141.

Mori, S., & Nishizawa, N. (1987). Methionine as a dominant precursor of phytosiderophores in Graminaceae plants. *Plant and Cell Physiology 28*(6): 1081-1092.

Nozoye, T. (2018). The nicotianamine synthase gene is a useful candidate for

doi:10.6342/NTU202301575

improving the nutritional qualities and Fe-deficiency tolerance of various crops. *Frontiers in plant science 9*: 340.

O'Dell, B. L., & Sunde, R. A. (1997). *Handbook of Nutritionally Essential Mineral Elements*. CRC Press.

Oppenheimer, S. J. (2001). Iron and its relation to immunity and infectious disease. *The Journal of Nutrition 131*(2): 616S-635S.

Ortiz-Monasterio, I., & Graham, R. (1999). Potential for enhancing the Fe and Zn concentration in the grain of wheat. Improving Human Nutrition through Agriculture: The role of International Agricultural Research. Proceedings of a Symposium. Los Baños, Philippines. 5-7 Oct.

Ozeki, H., Wakamatsu, K., Ito, S., & Ishiguro, I. (1997). Chemical characterization of eumelanins with special emphasis on 5, 6-dihydroxyindole-2-carboxylic acid content and molecular size. *Analytical Biochemistry 248*(1): 149-157.

Pamuk, G. E., Top, M. Ş., Uyanık, M. Ş., Köker, H., Akker, M., Ak, R., Yürekli, Ö. A., & Çelik, Y. (2016). Is iron-deficiency anemia associated with migraine? Is there a role for anxiety and depression? *Wiener Klinische Wochenschrift 128*(8): 576-580.

Prasad, R., Shivay, Y. S., & Kumar, D. (2014). Agronomic biofortification of cereal grains with iron and zinc. *Advances in Agronomy 125*: 55-91.

doi:10.6342/NTU202301575

Pugalenthi, M., Vadivel, V., & Siddhuraju, P. (2005). Alternative food/feed perspectives of an underutilized legume Mucuna pruriens var. utilis—a review. *Plant Foods for Human Nutrition 60*(4): 201-218.

Rajniak, J., Giehl, R. F., Chang, E., Murgia, I., von Wirén, N., & Sattely, E. S. (2018). Biosynthesis of redox-active metabolites in response to iron deficiency in plants. *Nature Chemical Biology 14*(5): 442-450.

Rasmussen, K. M. (2001). Is there a causal relationship between iron deficiency or iron-deficiency anemia and weight at birth, length of gestation and perinatal mortality? *The Journal of Nutrition 131*(2): 590S-603S.

Riley, P. A. (1997). Melanin. *The International Journal of Biochemistry & Cell Biology 29*(11): 1235-1239.

Römheld, V., & Marschner, H. (1983). Mechanism of iron uptake by peanut plants: I. FeIII reduction, chelate splitting, and release of phenolics. *Plant Physiology 71*(4): 949-954.

Römheld, V., & Marschner, H. (1986). Evidence for a specific uptake system for iron phytosiderophores in roots of grasses. *Plant Physiology 80*(1): 175-180.

Santi, S., & Schmidt, W. (2009). Dissecting iron deficiency-induced proton extrusion in Arabidopsis roots. *New Phytologist 183*(4): 1072-1084.

Schmid, N. B., Giehl, R. F., Döll, S., Mock, H.-P., Strehmel, N., Scheel, D., Kong,

doi:10.6342/NTU202301575

X., Hider, R. C., & von Wirén, N. (2014). Feruloyl-CoA 6′-Hydroxylase1-dependent coumarins mediate iron acquisition from alkaline substrates in Arabidopsis. *Plant Physiology 164*(1): 160-172.

Schmidt, H., Günther, C., Weber, M., Spörlein, C., Loscher, S., Böttcher, C., Schobert, R., & Clemens, S. (2014). Metabolome analysis of Arabidopsis thaliana roots identifies a key metabolic pathway for iron acquisition. *PloS One 9*(7): e102444.

Scibior, D., & Czeczot, H. (2006). Katalaza–budowa, właściwości, funkcje [Catalase: structure, properties, functions]. *Postepy Hig Med Dosw (Online) 60*: 170-180.

Shojima, S., Nishizawa, N.-K., Fushiya, S., Nozoe, S., Irifune, T., & Mori, S. (1990). Biosynthesis of phytosiderophores: *in vitro* biosynthesis of 2′-deoxymugineic acid from L-methionine and nicotianamine. *Plant Physiology 93*(4): 1497-1503.

Sillanpaa, M. (1997). Environmental Fate of EDTA and DTPA. 85–111. *Springer, New York, NY*.

Sisó-Terraza, P., Luis-Villarroya, A., Fourcroy, P., Briat, J.-F., Abadía, A., Gaymard, F., Abadía, J., & Álvarez-Fernández, A. (2016). Accumulation and secretion of coumarinolignans and other coumarins in Arabidopsis thaliana roots in response to iron deficiency at high pH. *Frontiers in Plant Science 7*: 1711.

Stansley, B. J., & Yamamoto, B. K. (2015). L-dopa and brain serotonin system

doi:10.6342/NTU202301575

dysfunction. *Toxics 3*(1): 75-88.

Steiner, U., Schliemann, W., & Strack, D. (1996). Assay for tyrosine hydroxylation activity of tyrosinase from betalain-forming plants and cell cultures. *Analytical Biochemistry 238*(1): 72-75.

Stoltzfus, R. J. (2003). Iron deficiency: global prevalence and consequences. *Food and Nutrition Bulletin 24*(4_suppl_1): S99-S103.

Sugumaran, M. (2002). Comparative biochemistry of eumelanogenesis and the protective roles of phenoloxidase and melanin in insects. *Pigment Cell Research 15*(1): 2-9.

Suzuki, M., Urabe, A., Sasaki, S., Tsugawa, R., Nishio, S., Mukaiyama, H., Murata, Y., Masuda, H., Aung, M. S., & Mera, A. (2021). Development of a mugineic acid family phytosiderophore analog as an iron fertilizer. *Nature Communications 12*(1): 1558.

Taalab, A., Ageeb, G., Siam, H. S., & Mahmoud, S. A. (2019). Some Characteristics of Calcareous soils. A review AS Taalab1, GW Ageeb2, Hanan S. Siam1 and Safaa A. Mahmoud1. *Middle East J 8*(1): 96-105.

Theil, E. C. (2003). Ferritin: at the crossroads of iron and oxygen metabolism. *The Journal of Nutrition 133*(5): 1549S-1553S.

Timberlake, C. (1964). 975. Iron–malate and iron–citrate complexes. *Journal of the*

doi:10.6342/NTU202301575

Chemical Society (Resumed): 5078-5085.

Ueno, D., Rombola, A., Iwashita, T., Nomoto, K., & Ma, J. (2007). Identification of two novel phytosiderophores secreted by perennial grasses. *New Phytologist 174*(2): 304-310.

Vélez-Bermúdez, I. C., & Schmidt, W. (2022). How plants recalibrate cellular iron homeostasis. *Plant and Cell Physiology 63*(2): 154-162.

Vivas, A., Marulanda, A., Ruiz-Lozano, J. M., Barea, J. M., & Azcón, R. (2003). Influence of a Bacillus sp. on physiological activities of two arbuscular mycorrhizal fungi and on plant responses to PEG-induced drought stress. *Mycorrhiza 13*(5): 249-256.

Wade, L., & Katzman, R. (1975). Synthetic amino acids and the nature of L-DOPA transport at the blood-brain barrier. *Journal of Neurochemistry 25*(6): 837-842.

Wang, J., & Blancafort, L. (2021). Stability and optical absorption of a comprehensive virtual library of minimal eumelanin oligomer models. *Angewandte Chemie 133*(34): 18948-18957.

Yanqun, Z., Li, Q., Fangdong, Z., Jiong, W., Yuan, L., Jianjun, C., Jixiu, W., & Wenyou, H. (2020). Intercropping of Sonchus asper and Vicia faba affects plant cadmium accumulation and root responses. *Pedosphere 30*(4): 457-465.

Zanin, L., Tomasi, N., Cesco, S., Varanini, Z., & Pinton, R. (2019). Humic

doi:10.6342/NTU202301575

substances contribute to plant iron nutrition acting as chelators and biostimulants. *Frontiers in Plant Science 10*: 675.

Zeng, H., Xia, C., Zhang, C., & Chen, L.-Q. (2018). A simplified hydroponic culture of Arabidopsis. *Bio-protocol*: e3121-e3121.

Zingore, S., Delve, R. J., Nyamangara, J., & Giller, K. E. (2008). Multiple benefits of manure: the key to maintenance of soil fertility and restoration of depleted sandy soils on African smallholder farms. *Nutrient Cycling in Agroecosystems 80*(3): 267-282.

doi:10.6342/NTU202301575